UNIVERSITÀ DEGLI STUDI DI NAPOLI "FEDERICO II"

Facoltà di Medicina e Chirurgia

Dottorato di Ricerca in Terapie Avanzate Biomedico-Chirurgiche

33° ciclo

Coordinatore Ch. mo Prof. Giovanni Di Minno

Dipartimento di Medicina Clinica e Chirurgia

Tesi di Dottorato

"Conventional and innovative replacement treatments in Adrenal iNsufficiency: Identification of new bioMArkers of Glucocorticoid Exposure "AN IMAGE"

The interplays between biological clocks, physiological and non-physiological cortisol exposure, metabolic and immune system: impact on morbidity and quality of life of patients with adrenal insufficiency

RELATORE:

Ch. mo Prof.

Rosario Pivonello

CANDIDATA:

Dott.ssa

Chiara Simeoli

ANNO ACCADEMICO 2020/2021

INDEX

Patients

Study medication and dose adjustments

Procedures

Outcomes

Statistical analysis

Results

5. **EX VIVO STUDY**

Study design

Participants

Study medication and dose adjustments

Procedures

Outcomes

Statistical analysis

Results

6. **DISCUSSION**
7. **POSSIBLE APPLICATION POTENTIALITIES**
8. **REFERENCES**
9. **FIGURES & TABLES**

1. INTRODUCTION

Circadian rhythm biological machinery

In 2017 the Nobel Prize for Physiology or Medicine was awarded to three American scientists, Jeffrey C. Hall, Michael Rosbash and Michael W. Young, for discovery of the circadian rhythm biological machinery. Since their seminal discovery, circadian biology has developed into a highly dynamic research field, with major implications for human health. Indeed, several physiological and behavioural processes are orchestrated by the circadian system, a powerful endogenous timing system functioning with a rhythmicity of 24 hrs cycles. The mammalian circadian system is regulated by a “master” clock, residing in hypothalamic suprachiasmatic nucleus, receiving information from external stimuli, defined “zeitgebers”, including light-dark and sleep-wake cycles, hunger-feeding-satiety circle, temperature shift, stressors, social cues, and activates responses aimed at synchronizing the peripheral clocks with exogenous and endogenous inputs.

Indeed, the “master” clock is connected to multiple “peripheral” clocks, represented by genes and proteins dislocated in several peripheral tissues.

“Master” and “peripheral” clocks have the same circadian machinery, which acts with a transcriptional/translational feedback loop mechanism, generating physiological circadian rhythms. The “canonical model” considers this loop to consist of a positive and a negative arm. The positive arm is composed by Bmal1 (brain-muscle ARNT-like protein 1) and Clock (Npas2 in neuronal tissue), two transcriptional activators promoting the transcription of Period (Per1, 2, 3) and Crypthocrome (Cry1, 2) genes, codifying for PER and CRY proteins, transcriptional repressors which represent the negative arm. PER and CRY inhibit Bmal1-Clock activity, therefore self-regulating their own transcription and closing the loop.

Particularly, Clock and Bmal1 heterodimerize and initiate transcription of target genes Per1, 2 and 3 and Cry1 and 2. Proteins PER and CRY translocate back to repress their own transcription, blocking Clock-Bmal1.

The interplay between the circadian rhythm biological machinery and metabolic and immune systems

The circadian machinery has been documented to regulate a series of functions related to various systems, including metabolism and immune system. Indeed, several metabolic and immune cell models, express the circadian machinery, including mouse hepatocytes and adipocytes, as well as human monocytes/macrophages, T and B lymphocytes and dendritic cells.

Consistently, circadian rhythm disruption has been associated with metabolic and immune disorders in *in vivo* studies on either animal or human models: Bmal-1 knockout (KO) mice developed glucose intolerance or diabetes, with the increase in fasting glucose levels accompanied by a reduction in insulin secretion, due to an impairment in insulin secretion pathway in pancreatic β-cells. Clock mutant mice developed not only hyperphagia, associated with upregulation of two potent orexigenic peptides, orexin and ghrelin, and consequent obesity associated with hyperleptinemia, but also hyperglycemia and hyperlipidemia. Per2 KO mice developed hyperphagia, likely consequent to the loss of circadian feeding rhythm leading to equal food intake during both the light and dark daytime, and consequent obesity.

Additionally, Bmal-1 and Clock KO mouse models showed increased susceptibility to lipopolysaccharide endotoxin shock, and diminished pro-inflammatory cytokines production.

Recently, an increasing bulk of translational studies has reinforced these preclinical evidences. In humans, a Cry2 allele variant, due to a single nucleotide polymorphism, has been associated with impairment of glucose tolerance or diabetes in the general population of European and Asiatic cohorts of subjects. Moreover, a circadian rhythm misalignment, obtained by forcing behavioral habits of healthy male subjects with an abrupt shifting of their normal circadian rhythm by 12 hrs, impairs skeletal muscle insulin sensitivity, with consequent increase of fasting glucose, due to decreased insulin-stimulated glucose disposal and uptake. Interestingly, a study on adipose tissues derived from a population of obese women demonstrated that adipocyte non-physiological fluctuation components belonging to the circadian clock, represented by increased circadian variability of BMAL1 and PER2 expression, was associated with an increased sagittal diameter of the respective women abdomen, marker of visceral obesity, demonstrating that the impairment of the circadian clock might be associated with metabolic syndrome.

The interplay between the circadian rhythm biological machinery and hypothalamus-pituitary-adrenal axis

In humans, SCN cells cyclically stimulate paraventricular nucleus (PVN) neurons, through direct and indirect axonal projections, leading to a circadian release of cortisol-releasing hormone (CRH) and, consequently, adrenocorticotropic hormone (ACTH) and cortisol, the main endogenous GC, which, in turn, contributes to trigger oscillation of peripheral clocks. Indeed, the circadian clock regulates cortisol secretion, rhythm and action, acting at different levels of the hypothalamus-pituitary-adrenal (HPA) axis, including at the level of glucocorticoid (GC) receptors, whereas GCs are able to modulate the activity of the

circadian clock, through the regulation of the expression and oscillation rhythm of clock genes and proteins, in a reciprocal interplay.

Circulating GC levels fluctuate according to a circadian rhythm, reaching their zenith in the early morning, and their nadir in the late evening. Diurnal circadian oscillation of circulating GCs contributes to influence peripheral clock genes expression, acting as “endogenous zeitgeber”.

Therefore, impaired GC rhythmicity could negatively affect morbidity and mortality in patients with HPA axis disorders, such as hypercortisolism (Cushing’s Syndrome, CS) or hypocortisolism (adrenal insufficiency, AI), which, therefore, represent interesting models to study the effects of GC circadian rhythm disruption.

CS is a serious clinical condition caused by endogenous or exogenous GC excess. The loss of GC circadian rhythm is one of the most common and specific features of the disease. The syndrome is associated with increased mortality, mainly due to cardiovascular and infectious diseases, and impaired quality of life (QoL), because of the occurrence of several comorbidities. These clinical complications include a peculiar type of metabolic syndrome, consisting of visceral obesity, systemic arterial hypertension, impairment of glucose metabolism, and dyslipidaemia.

In CS, metabolic syndrome is strictly associated with cardiovascular disorders, including vascular atherosclerosis and cardiac damage, which, together with haemostatic disorders, responsible for a thrombosis diathesis, contributes to the increased cardiovascular risk. Additionally, CS patients display a severe hindering of immune response, mainly consisting of immune deficits leading to increased mortality and/or hospitalization rate, especially due to the increased frequency and severity of infectious diseases and sepsis. These infectious complications, historically attributed to GC excess, have recently

appeared significantly influenced by impaired CG rhythmicity, although the involved mechanisms should be further investigated.

On the other side of the moon, AI is a rare endocrine disorder characterized by cortisol deficiency and by a complete loss of cortisol circadian rhythm. AI patients need life-long GC replacement therapy to replace cortisol deficiency. In the 1950s, with the GC replacement therapy introduction, AI patients began to have a nearly normal lifespan.

Among the various GC formulations, immediate-release hydrocortisone (IR-HC), cortisone acetate, prednisone and prednisolone are the most common used. Mineralocorticoid replacement is achieved with fludrocortisone.

GC dose and timing adjustments are the main challenges to avoid the imbalance between overtreatment, causing the unwanted adverse effects of exogenous GC over-replacement, mainly including obesity, dyslipidaemia, glucose intolerance, insulin resistance, metabolic syndrome, cardiovascular diseases, osteopenia and osteoporosis, infertility, impaired QoL and health status, and under-treatment, with the risk of developing adrenal crises.

Beyond replacing cortisol deficiency, the aim of the GC replacement therapy is to replicate the physiological cortisol circadian rhythm.

Conventional formulations appear still inadequate to mimic cortisol circadian rhythm. Indeed, in the last years, in AI patients under conventional GCs, several evidences have hypothesized that GC circadian rhythm disruption, represented by non-physiological pattern of peaks and troughs and elevated evening GC levels, might be responsible for the increased risk of visceral obesity, metabolic syndrome, glucose intolerance and insulin resistance, coronary artery calcifications, immune dysfunctions, as well as insomnia, QoL impairment and increased mortality.

More recently, a once daily dual-release HC (OD-DR-HC) formulation, named Plenadren®, based on an immediate release coating, responsible of the morning cortisol peak, and an

extended release core, responsible of the prolonged cortisol release during the day, aimed at better mimicking the normal physiological cortisol circadian rhythm, has been evaluated in AI patients.

In an open, randomized, two-period, 12-week crossover multicenter trial with a 24-week extension at five university hospital centres, this new formulation was shown to induce a serum cortisol profile similar to healthy subjects, with an overall reduction of 20% in cortisol levels, compared with IR-HC thrice daily. Several studies demonstrated that OD-DR-HC was able to induce a significant improvement in body weight, body mass index (BMI), waist circumference, blood pressure, lipid, glucose and bone profiles as well as QoL. This treatment was also proved to be safe and well-tolerated during long term treatment.

The described clinical complications observed in CS and AI are similar to those reported in humans with GC circadian disruption, such as night shift workers, and in chronic stress. Indeed, night shift workers reported metabolic syndrome, obesity, diabetes and cardiovascular diseases. Similarly, under conditions of shift work, cytokine secretion and immune cell counts are disturbed, leading to a desynchronization of rhythmic immune parameters, contributing to the increased risk for infectious and autoimmune diseases. Likewise, subjects exposed to high late afternoon, evening and nocturnal GC levels reported glucose intolerance, decreased insulin sensitivity, visceral obesity and coronary calcifications.

Therefore, understanding GC circadian rhythm disruption mechanisms might be of utmost relevance in the management of CS and AI patients, by upsetting the hard and exiting challenges. The comprehension and characterization of the involved mechanisms might

greatly reduce metabolic, cardiovascular and immune morbidity and mortality, and improve QoL of patients.

These discoveries might provide innovative insights overlooking to prevention strategies and tailored therapies to the millions of subjects with GC circadian disruption.

2. AIMS

Since physiological GC levels have been shown pivotal in synchronization of central and peripheral clocks, the hypothesis of the current study is that an anti-circadian rhythm or an abnormal sequence of GC peaks and nadirs could trigger several re-synchronization processes, leading to metabolic and immune systems disruption.

This study describes the interplays between biological clocks, physiological and non-physiological cortisol exposure and metabolic and immune system both in *in vitro*, *in vivo* and *ex vivo* models, evaluating the impact on morbidity and QoL of patients with AI.

This study has included three parts: an *in vitro* and an *in vivo* studies conducted at the Department of Clinical Medicine and Surgery, Federico II University of Naples, and an *ex vivo* study conducted in collaboration with the Department of Experimental Medicine, Sapienza University of Rome.

3. IN VITRO STUDY

Aim

The current *in vitro* study aims at exploring the molecular effects of physiological and non-physiological HC concentrations, administered in different time-points of circadian rhythm, on insulin sensitivity in an experimental model of mouse skeletal muscle cell.

Study design

The model used for the study is a mouse skeletal muscle cell line, the C2C12 myocytes appropriately obtained by the differentiation of respective myoblasts; this model is usually assessed for *in vitro* studies on cell proliferation, but also on glucose uptake and utilization, glycogen synthesis, insulin response, mitochondrial activity, protein synthesis, glucose and fatty acids oxidation, as well as skeletal muscle contractile activity.

The study protocol initially required C2C12 myocytes synchronization, a process by which *in vitro* cells can assume an autonomous and self-sustained circadian expression of components of circadian clock. The synchronization has been performed by a serum shock protocol and has been verified by following the oscillation of clock genes expression every 4 hrs for a consecutive 24 hrs interval of time, in order to set the time-points of exposure to HC.

Although a mouse cell model, C2C12, was used for the current study, HC, and not corticosterone, was administered for the *in vitro* experiments to better mimic the human condition, without affecting the experimental results having HC and corticosterone the same binding affinity for glucocorticoid receptor (GR).

The main experiment was based on the exposure of the C2C12 myocytes to different HC concentrations in the different time-points of the circadian rhythm of the synchronized cells and to measure the effects on insulin sensitivity.

The aspects of insulin sensitivity evaluated during the experiments were: 1) a general analysis of insulin sensitivity, performed by the evaluation of gene expression profile through RT-qPCR insulin resistant-related array, investigating the simultaneous expression levels of 84 key genes involved in the cell mechanisms regulating insulin sensitivity, and consequently involved in the development of insulin resistance; 2) a specific analysis of insulin receptor signaling, the main determinant of insulin sensitivity, performed by the evaluation of gene expression profile through RT-qPCR; and 3) a specific analysis of crucial intracellular mechanisms associated with insulin sensitivity, performed by the evaluation of protein expression through western blot. On the basis of the results obtained at genomic level, the mechanisms investigated through western blot included not only the pathways strictly related to the insulin receptor signaling, but also a specific aspect of lipid metabolism, which is the fatty acid β-oxidation, a catabolic process through which fatty acids are degraded to trigger citric acid cycle and produce energy, and whose impairment exacerbates insulin sensitivity by inducing a lipotoxic and inflammatory state, detrimental for intracellular insulin signal in skeletal muscle.

Cell line

C2C12, a mouse skeletal muscle cell line, is an adherent diploid sub-clone of the mouse myoblast cell line established by David Yaffe. C2C12 cell line was purchased from ATCC® (CRL-1772™) and cultured in base medium Dulbecco's Modified Eagle's Medium (DMEM) with 10% of fetal bovine serum (FBS) and $1*10^5$ U/L penicillin/streptomycin in a humidified condition in 5% CO_2 at 37°C. After 2 days of adhesion, $3*10^5$ C2C12 cells were seeded in 60 mm dishes and terminally differentiated to myocytes by switch to a differentiating medium (DMEM with 2% of horse serum (HS), $10*10^5$ U/L penicillin/streptomycin, 1% insulin, transferrin, selenium [ITS]) for 48 hrs.

Cell synchronization

C2C12 terminally differentiated to myocytes, were synchronized by switching to a DMEM supplemented with 50% HS, capable to induce a serum shock. After 2 hrs in serum-rich DMEM, cells were rinsed and re-fed with serum-free DMEM for 24 hrs. At the established time-points (every 4 hrs over a 24 hrs period) dishes were washed twice with ice-cold PBS 1X, lysed, and harvested in 1 mL TRIzol reagent (Life Technologies, Carsbald, California, United States) by scraping with a rubber policeman and RNA extracted from cell lysates. To verify cell synchronization, messenger oscillation of the molecular circadian clock components Bmal1, Clock, Per1, Per2, Cry2 and protein oscillation of the molecular circadian clock component BMAL1, PER1, PER2, CRY2 were monitored during the 24 hrs period. The protein oscillation of CLOCK was not evaluated in the current study, since a previous *in vivo* study demonstrated that Clock KO mouse models continue to exhibit a stable and autonomous peripheral circadian rhythm suggesting that CLOCK is not essential for the proper functioning of the transcriptional and translational feedback loop of the circadian clock. **Figure 1** schematically shows the serum shock protocol used for the cell synchronization.

RNA isolation and RT-qPCR

Total RNA was extracted using TRIzol reagent (Life Technologies, Carsbald, California, United States). After cell centrifugation at 4°C to obtain the cell pellet, TRIzol was added to C2C12 pellet on ice and the pellet was carefully homogenized with pipet in eppendorf. After 15 min at room temperature (RT), 200 µl of chloroform were added and the eppendorf vortexed for 15 sec for 2 times with a pause of 2 min at RT. The mixture obtained was centrifuged at 12000xg for 15 min at 4°C and upper phase carefully transferred in a new clean eppendorf at RT. After measuring the volume obtained, a quantity of isopropanol equal to the half of the volume obtained and 1 µl of glycogen were

added and the sample preserved overnight at -20°C. The day after, the sample was centrifuged at 12000xg for 10 min at 4°C and the supernatant eliminated with pipet. The pellet was washed with 1 ml 75% ethanol and centrifuged at 12000xg for 5 min at 4°C. This passage was repeated three times. Lastly, the pellet was dried for 10 min in sterile condition at RT and 20 µl RNAse-free/sterile H_2O were added keeping the samples at 4°C for 1 h. The dissolved pellet was then heated for 5 min at 65°C, its purity assessed by the A260/A230 absorbance ratio and the samples stored at -80°C until use. The cDNA synthesis was performed using the RT2 First Strand Kit, purchased from Qiagen® (Milan, Italy); this protocol requires a first treatment for 5 min at 42°C followed by 2 min on ice with buffer GE (5X genomic DNA elimination buffer) to eliminate potential genomic DNA contamination and, subsequently, a retro-transcription process for cDNA synthesis.

In detail, starting from 1 µg RNA, the reverse transcription mix was prepared according to the manufacture's instruction. The mix was incubated for 15 min at 42°C and subsequently, immediately stopped by incubation at 95°C for 5 min. To each reaction 180 µl RNase-free water were added and the sample of cDNA stored at -20°C until use. The cDNA was used for quantification of messenger levels of the clock genes under investigation for the study. The total reaction volume (12.5 µl) consisted of 5 µl of cDNA, 7 µl of TaqMan® Universal PCR Mastermix (Applied Biosystems, Branchburg, NJ, USA) and 0.5 µl of primers-probes (Applied Biosystems, Branchburg, NJ, USA). RT-qPCR was performed with StepOne Plus Real-Time PCR System, using the standard protocol; briefly, after two initial heating steps at 50°C (2 min) and 95°C (10 min), samples were subjected to 40 cycles of denaturation at 95°C (15 sec) and annealing at 60°C (60 sec). All samples were assayed in duplicate. Values were normalized against the expression of the housekeeping gene 18S ribosomal RNA (18S). The relative expression of target genes was calculated using the comparative threshold method, denominated $2^{-\Delta Ct}$. To exclude

contamination of the PCR mixtures, in parallel with cDNA samples, reactions were also performed in the absence of cDNA template.

Drug

HC was purchased from Sigma Aldrich (Sigma Aldrich, Italy) and dissolved in 100% ethanol (EtOH). Stock solutions of HC at the concentration of 10^{-3} M were stored at -80°C and freshly thawed prior the experiments. Serial dilutions were prepared in serum-free DMEM as recommended by manufacturer.

Setting of time-points treatment

To establish the time-points of HC exposure, the beginning of the circadian cycle (Time 0 [T0]) was set with the beginning of serum shock and consistently with the “canonical model”, time-points treatment were established on the basis of clock genes circadian expression and in particular of Bmal1 messenger expression. The Bmal1 peak transcription level (acrophase), corresponding to the nadir of Per and Cry transcription levels, was considered to correspond to the early morning; conversely, the Bmal1 nadir transcription level (bathyphase), corresponding to the Per and Cry peak transcription levels, was considered to correspond to the early evening in the daily rhythm. Time-point with medium Bmal1 transcription level (midphase) was considered to resemble the afternoon in the daily rhythm.

Hydrocortisone treatment schedule

HC concentrations administered to C2C12 cells corresponded to the mean serum cortisol concentrations observed in healthy human subjects and AI patients treated with OD-DR-HC and with thrice-daily of conventional IR-HC. At the time-points of the cell circadian rhythm corresponding to 8 am, 1 pm and 6 pm of the subjective daily rhythm, C2C12 cells

were exposed for 1 h (minimum time to observe GC genomic effects and maximum time to avoid drastic cells de-synchronization) to different HC concentrations.

HC concentrations used to mimic physiological circulating cortisol concentrations (standard cortisol profile) have been reported in the text as “treatment schedule A” (TSA), while concentrations used to mimic the circulating cortisol concentrations reached in AI patients treated with OD-DR-HC were reported as “treatment schedule B” (TSB) (flat cortisol profile), and concentrations used to mimic the circulating cortisol concentrations reached in AI patients treated with thrice-daily of conventional IR-HC were reported as “treatment schedule C” (TSC) (steep cortisol profile) specifically at acrophase, midphase and bathyphase.

Figure 2 shows a simplified representation of the *in vitro* HC exposure at different circadian time-points.

Table 1 shows the treatment schedules and the correspondence to the time-points of the circadian rhythm obtained after C2C12 synchronization.

RT-qPCR insulin resistance-related array

RT2 Profiler PCR Array provided in 96-well plates, contained primer assays for 84 insulin resistance-related genes and 5 housekeeping genes (Mouse RT2 Profiler™ PCR Array Insulin Resistance kit, PAMM-156Z, Qiagen, Milan, Italy). In addition, 1 well contained a genomic DNA control, 3 wells contained reverse-transcription controls and 3 wells contained positive PCR controls. RT2 Profiler PCR Arrays were performed following the manufacturer’s recommendations. After centrifugation of RT2 SYBR® Green/ROX qPCR Mastermix (Qiagen, Milan, Italy), the PCR components were prepared in a 15 ml tube by adding 1250 µl 2X RT2 SYBR® Green qPCR Mastermix, 200 µl cDNA, 1050 µl H_2O and dispensing 25 µl of this mix to each well of MicroAmp® Fast Optic 96-well (Applied Biosystem, Lincoln Centre Drive Foster City, United States) in order to charge 10 ng cDNA

per well. The last six wells, containing positive controls, were charged with PCR components and RNase-free water. The plate was placed in StepOne Plus Real-Time PCR System, using a standard protocol; briefly, after two initial heating steps at 50°C (2 min) and 95°C (10 min), samples were subjected to 40 cycles of denaturation at 95°C (15 sec) and annealing at 60°C (60 sec). All samples were assayed in duplicate. Values were normalized against the arithmetic media of 5 housekeeping genes expression. Results are expressed as mean of three different experiments. Data analysis and validation were performed using the free online software provided by the manufacturer's website (Qiagen, Milan, Italy).

The insulin resistance-related array constituted by 84 insulin resistance-related genes was analyzed; genes could be categorized according to their specific function as follows: insulin signaling; non-insulin dependent diabetes mellitus; adipokine signalling; adipokines; receptors & transporters; signaling downstream of adipokines; innate immunity; inflammation; apoptosis; metabolic pathways, including carbohydrate metabolism, lipid metabolism, metabolite transport, infiltrating leukocyte markers of macrophages, Th1 cells and Th2 Cells.

Genes expression levels were considered significantly modified (upregulated or downregulated) if absolute fold change of relative gene expression >2.0 and p-values <0.01 were detected.

RT-qPCR genes variation validation

On the basis of RT-qPCR array gene expression changes, genes mainly involved in the skeletal muscle insulin receptor signaling, whose expression was determinant of insulin sensitivity, were chosen and validated through RT-qPCR in Sybr Green.

The total reaction volume (25 µl) consisted of 2 µl of cDNA, 12.5 µl of RT2 SYBR® Green/ROX qPCR Mastermix (Qiagen, Milan, Italy), 0.5 µl of primers-probes (Applied Biosystems, Branchburg, NJ, USA) and 10 µl of H_2O.

RT-qPCR was performed with StepOne Plus Real-Time PCR System, using the standard protocol; briefly, after two initial heating steps at 50°C (2 min) and 95°C (10 min), samples were subjected to 40 cycles of denaturation at 95°C (15 sec) and annealing at 60°C (60 sec). All samples were assayed in duplicate. Gene expression levels were normalized against the expression of the housekeeping gene cyclophilin A.

The relative expression of target genes was calculated using the comparative threshold method, $2^{-\Delta Ct}$. To exclude contamination of the PCR mixtures, in parallel with cDNA samples, reactions were also performed in the absence of cDNA template.

Protein isolation and Western Blot analysis

C2C12 myocytes were seeded at a density of $3*10^5$ in 60 mm dishes and terminally differentiated for 48 hrs after 2 days of adhesion. After HC treatment, cells were lysed, and protein extracted as previously described. Proteins from cell preparations were separated by 8% (according to protein's molecular weight to detect) SDS-PAGE and then electroblotted onto a nitrocellulose membrane for 1h in a TransBlot Bio-Rad apparatus. After a blocking treatment for 1h with 5% of milk, the nitrocellulose filters were probed overnight with primary antibodies specific for BMAL1 (#14020, Cell Signalling, Italy), PER1 (sc-398890, Santa Cruz Biotech, Inc), PER2 (GT5310, ThermoFisher, Italy), CRY2 (PA5-13125, ThermoFisher, Italy) to evaluate cell synchronization and confirm clock genes expression. Moreover, the molecular mechanisms investigated through western blot included not only the pathways strictly related to the insulin receptor signaling by analyzing intracellular levels of pIRS1 (Tyr608) (#09-432, Millipore, Italy), IRS1 (#2382, Cell Signalling, Italy), pAKT (Ser473) (#9271, Cell Signalling, Italy), AKT (#9272, Cell

Signalling, Italy), but also the fatty acid β-oxidation catabolic process, which contributes to exacerbate skeletal muscle insulin sensitivity, by analyzing intracellular levels of pAMPKα (Thr172) (40H9) (#2535, Cell Signalling, Italy), AMPKα (#2793, Cell Signalling, Italy), pACC (Ser79) (D7D11) (#11818, Cell Signalling, Italy), ACC (C83B10) (#3676, Cell Signalling, Italy). β-ACTIN (A4700; Sigma Aldrich, Italy) was used as endogenous control for protein expression analysis. Subsequently, filters were hybridized with peroxidase-conjugated secondary antibodies and immunoreactive bands were detected by ECL system. After chemiluminescent reaction, the blot was exposed to ImageQuant Las 4000 (GE Healthcare). Densitometry bands quantification was performed through ImageJ software.

Statistical analysis

All the experiments were replicated at least three times.

Statistical analyses of clock gene expression and C2C12 cells synchronization were performed using GraphPad Prism 5 software.

Cosinor analysis was used to calculate the 24 hrs rhythmicity and to graphically reproduce the presence of 24 hrs oscillations of clock genes across different time-points. In detail, Cosinor analysis was performed by fitting a periodic sinusoidal function $f(t)= M+Acos(t\pi /12- \Phi)$ to the expression value of each gene across the time-points, where $f(t)$ is the gene expression levels in a given time-point, *M Mesor* is the midline estimating statistic of mean, A is the sinusoidal amplitude of oscillation, t is the time expressed in hrs and Φ is the acrophase (peak time of the fitted cosine function). P values depicted in each graph were calculated by ANOVA. The expression of individual messenger by RT-qPCR array was analyzed using threshold cycle (Ct) values obtained with a threshold of 0.4. Ct values of 35 or greater for any messenger in either the control or the experimental samples was excluded from the analysis and marked as undetectable or undetermined.

Data analysis was performed uploading the Ct values that passed through these stringent criteria on Qiagen web portal (*https://dataanalysis.qiagen. com/pcr/arrayanalysis.php; Qiagen, Milan, Italy*). Dose-time comparison of fold change were calculated by the software using the ΔΔCt method, calculating the fold change in terms of C_t values in each group of treatment, and relativized on five housekeeping genes expression levels.

The Volcano plot analysis, combining the measure of statistical significance from the statistical test with the magnitude of the fold change, was used to evaluate the significant genes expression change. Gene expression levels were considered significant modified (upregulated or downregulated) whether absolute fold change of relative gene expression >2.0 and p-values <0.05 were detected. Features of interest are typically those in the upper left- and right-hand corners of the Volcano plot, as these have large fold changes (lie far from x=0) and are statistically significant (have large y-values). Validation of downregulated genes, evaluated by RT-qPCR, was analyzed through ANOVA analysis followed by a multiple comparative test (Bonferroni, Newman-Keuls or Dunnett's correction).

Results

C2C12 cells, after a suitable synchronization, displayed a different response to the different doses of HC, depending on the time of exposure, particularly on the time-point of the cell circadian rhythm.

Rhythmic expression of clock genes in synchronized C2C12 cells

The synchronization procedure clearly induced oscillation of the clock genes. Messenger expression of Bmal1 peaked at 12 hrs and decreased, reaching the nadir, at 20 hrs time-points. Similarly, protein expression of BMAL1, that reached the highest levels at 12 hrs and the lowest levels around 20 hrs time-points. Clock messenger expression, although

following a cyclic pattern, exhibited little periodicity. Conversely, messenger and protein expression of Per1, Per2 and Cry2 genes peaked at 24 hrs and decreased, reaching the nadir, at 12 hrs. Based on these results and according to the commonly accepted circadian clock model, in order to set the *in vitro* exposure times, it has been assumed that the 12 hrs time-point correspond to the early morning (Bmal1 acrophase), 15 hrs time-point roughly correspond to the afternoon (Bmal1 midphase) while 20 hrs time-point represents the early evening of the daily rhythm (Bmal1 bathyphase).

Figure 3A shows the messenger expression profile of the clock genes during the 24 hrs period, whereas **Figure 3B** shows the protein expression profile of the clock genes during the 24 hrs.

Expression analysis of 84 insulin resistance-related genes in synchronized C2C12

HC concentrations used to mimic circulating cortisol concentrations reached in AI patients treated with OD-DR-HC (TSB) (flat cortisol profile) or treated with thrice-daily of conventional IR-HC (TSC) (steep cortisol profile) were compared each other and to HC concentrations used to mimic physiological circulating cortisol concentrations (TSA) (standard cortisol profile).

In the acrophase, TSB and TSC produced no relevant changes in the expression of various genes when compared to TSA or reciprocally. **Figure 4A, 4B and 4C** show the volcano plot representations without significant gene expression changes after TSA, TSB and TSC in the acrophase.

In the midphase, TSB and TSC produced minor changes in the expression of various genes when compared to TSA or reciprocally. **Figure 5A, 5B and 5C** show the volcano plot representations without significant gene expression changes, except for Cs and Il18r1, after TSA, TSB and TSC in the midphase.

In the bathyphase, TSB and TSC produced a significantly different effect on expression of various genes when compared to TSA or reciprocally. Indeed, no significant change in gene expression has been detected when TSB was compared to TSA, whereas 38 different genes were downregulated and 1 gene was upregulated, when TSC was compared to TSA. **Figure 6A, 6B and 6C** show the Volcano plot representations of gene expression changes after TSA, TSB and TSC in the bathyphase. Particularly, **Figure 6B** and **Figure 6C** show the significant gene expression changes after TSB and TSC comparing to TSA in the bathyphase. Among the 39 regulated genes, the Volcano plot analysis revealed the significant downregulation of 21 genes. **Table 2** details 21 genes significantly downregulated specifying fold changes and p-values.

Similarly, 34 genes were downregulated when TSB was compared to TSC. Among the 34 regulated genes, the Volcano plot analysis revealed a significant downregulation of 22 genes, with a superimposable profile observed comparing TSC and TSA. **Table 3** details 22 genes significantly downregulated specifying fold changes and p-values.

Among the genes significantly regulated during bathyphase when TSB and TSC were compared to TSA and reciprocally, as detailed above, Insr, Irs1, Irs2, Pi3kca and Adipor2 gene expression were validated through Sybr Green RT-qPCR. No change in gene expression has been detected when TSB was compared to TSA, while when TSC was compared to TSA a strong and significant inhibition of Insr (**p<0.01), Pi3kca (****p<0.0001) and Adipor2 (**p<0.01) expression and a marked, but not significant, inhibition of Irs1 and Irs2 occurred. **Figure 7** shows the expression levels of Insr, Irs1, Irs2, Pi3kca, Adipor2 after TSA, TSB and TSC in bathyphase.

Analysis of intracellular insulin receptor signaling and fatty acid β-oxidation pathway

Considering the huge and different effect observed on gene expression and induced during the bathyphase by TSB and TSC compared to TSA, the analysis of intracellular

proteins involved in insulin sensitivity, particularly in insulin receptor signaling and in fatty acid β-oxidation pathway has been performed only in C2C12 during the bathyphase.

TSB and TSA induced similar intracellular protein modifications. Conversely, TSC strongly affects intracellular insulin receptor signaling and fatty acid β-oxidation pathway.

Figure 8 shows that TSC inhibited IRS1 phosphorylation at Tyr608 and AKT phosphorylation at Ser473, as well as AMPKα phosphorylation at Thr172 and ACC phosphorylation at Ser79.

Figure 9 shows a graphic representation of the investigated intracellular insulin receptor signaling and fatty acid β-oxidation pathway in the skeletal muscle.

4. IN VIVO STUDY

Study design

A 12-month open-label, non-randomized intervention study was conducted at the Department of Clinical Medicine and Surgery, Federico II University of Naples.

The study was approved by the local ethics committee of Federico II University of Naples and complied with the Declaration of Helsinki, in line with the Guidelines for Good Clinical Practice.

Patients

Eligible patients were aged 18–80 years, had a previously established diagnosis of primary or secondary AI, were taking conventional GC therapy, consisting in cortisone acetate or IR-HC in a twice or thrice daily regimen. Patients were treated with once daily doses of fludrocortisone as needed. All patients were stably treated for at least 3 months before enrolment, and were willing to change their regimen.

Exclusion criteria included patients younger than age 18 and higher than age 80, a significant psychiatric illness, a history of alcohol and drug abuse, gastrointestinal emptying or motility disturbances (i.e. chronic diarrhoea), therapy with hepatic enzyme induction drugs interfering with GC metabolism, or immunosuppressive steroid therapy.

All subjects were recruited in the order they appeared chronologically for their routine visit in the outpatient clinic of the Department of Clinical Medicine and Surgery, Section of Endocrinology, Federico II University of Naples, from 1st February 2018 to 30th September 2019. Patients were followed-up to 30th September 2020.

All patients provided written informed consent before entering the study, with respect to study participation, and confidentiality statement of data collection according to the Italian privacy policy. All data were anonymised.

Twenty patients (12 F, 8 M, 48.6 ± 14.1 yrs, 20-66 yrs) were enrolled in the study.

Six of these 20 patients discontinued the study. Reasons for dropout were patient's decision. Therefore, fourteen patients (8F, 6M, 48.85 ± 15.69 yrs, 20-66 yrs) were included in the primary analysis. Particularly, seven patients suffered from primary AI (5 F, 2 M, 41.8 ± 15.5 yrs, 21-60 yrs), and seven from secondary AI (3 F, 4 M, 51.85 ± 15.26 yrs, 20-66 yrs).

At study entry 11 patients were treated with cortisone acetate at the dose of 44.3 ± 12.6 mg/day, and particularly 8 (72.8%) patients in a twice daily regimen and 3 (27.2%) patients in a thrice daily regimen. Three patients were treated with IR-HC at the dose of 28 ± 3.5 mg/day, all treated in a thrice daily regimen. Six patients were treated with fludrocortisone at the dose of 0.1 ± 0.05 mg/day, in a once-daily regimen.

All patients were switched to OD-DR-HC at the dose of 31.78 ± 6.68 mg/day, entered the study and were evaluated before and 12 months after the switch to OD-DR-HC.

Study medication and dose adjustments

At baseline all patients were instructed to take the first dose on waking before leaving their bed and subsequent doses according to their established schedule (two or three times a day), but with the last dose no later than 6 pm.

Patients allocated to OD-DR-HC were instructed to take the dose on waking, before leaving their bed.

For all participants, blood samples were collected in the morning, between 8 and 9 am, by research nurses after overnight fasting; participants had to take their usual morning dose 3 hrs before blood sampling.

Patients previously on multiple doses of IR-HC a day received the same total daily dose, whereas patients previously on cortisone acetate received 0.8 mg of HC per 1 mg of cortisone, as recommended by the European Medicines Agency drug fact sheet. Intermediate doses were rounded up to the nearest 5 mg (eg, 22.5 mg to 25 mg) to avoid any potential dangerous reduction in total daily dose.

All patients treated with fludrocortisone at study entry maintained their treatment also after OD-DR-HC switch.

No change was allowed in any other medication or in GC dose or timing, except for in cases of intercurrent illnesses requiring upscaling of the dose, and only after consultation with the study team. Before entering the study, all patients received a steroid emergency card and special teaching regarding intercurrent illnesses and adrenal crisis. In case of less severe intercurrent illnesses the oral OD-DR-HC daily dose was doubled (a second dose 8 hrs after the first dose), whereas in case of severe intercurrent illnesses the oral regimen was replaced by the parental one.

All patients were interviewed about their dietary habits and all were on a standard Mediterranean diet. General nutritional recommendations were provided.

Procedures

All investigations were performed by a central laboratory at Federico II University of Naples.

Metabolic parameters assessment

Body weight (BW), BMI, waist circumference (WC), sistolic blood pressure (SBP) and diastolic blood pressure (DBP) were assessed at the baseline and 12 months after the switch to OD-DR-HC.

In particular, BW was measured using a calibrated balance, and height was recorded at baseline; these measurements were used to calculate BMI. WC was measured midway between the palpated iliac crest and lowest rib margin in the left and right mid-axillary line.

SBP and DBP were recorded in sitting posture after a 5 min rest.

Total, low density lipoprotein (LDL) and high-density lipoprotein (HDL) cholesterol, triglycerides, fasting plasma glucose (FPG), fasting insulin, glycated haemoglobin (HbA1c) were performed according to standard procedures.

In the entire cohort of 11 patients, with the exception of the three patients with a previous diagnosis of diabetes mellitus, a standard oral OGTT was performed according to standard published protocols, after a 10-h fast, on separate days, not assuming GC therapy before blood samples. Briefly, 75 g of glucose was ingested over 5 min and samples for glucose and insulin measurements were taken at 0, 30, 60, 90, and 120 min. AUC glucose and insulin were calculated with the trapezoidal rule. Insulin resistance and sensitivity were estimated using the homeostasis model assessment (HOMA) index, Matsuda Index, and the Insulin Sensitivity Indexes (ISI) 0',120' calculated according to available formulas, using glucose and insulin values obtained from the OGTT.

According with BMI, patients were classified in three groups: normal weight (BMI < 25 kg/m^2), overweight (BMI ≥ 25 and < 30 kg/m^2) and obese (BMI ≥ 30 kg/m^2).

Visceral obesity was defined as WC ≥ 94 cm in men and ≥ 80 cm in women, according with IDF criteria.

Systemic arterial hypertension was defined as SBP ≥140 mmHg and/or DBP ≥90 mmHg, according to the American Society of Hypertension and the International Society of Hypertension guidelines, or treatments of a previously diagnosed systemic arterial hypertension.

The lipid profile was evaluated according to the ATP-III guideline criteria. Hypercholesterolemia was defined as total cholesterol ≥ 200 mg/dl (≥ 5.17 mmo/L) or LDL-cholesterol ≥ 130 mg/dl (≥ 3.36 mmo/L) or HDL-cholesterol < 40 mg/dl (<0.9 mmo/L) in men and < 50 mg/dl (1.1 mmol/L) in women, or specific treatments for these lipid abnormalities. Hypertriglyceridemia was defined as triglycerides ≥ 150 mg/dl (≥ 1.7 mmo/L) or specific treatments for this lipid abnormality. The diagnosis of Impaired Fasting Glucose (IFG), Impaired Glucose Tolerance (IGT) and diabetes mellitus was performed according to the latest American Diabetes Association guidelines. IFG was diagnosed if FPG was between 100 and 125 mg/dl (5.6-6.9 mmol/L). IGT was diagnosed if a two hrs plasma glucose after Oral Glucose Tolerance Test (oGTT) was 140-199 mg/dl (7.84-11 mmol/L). Diabetes mellitus was defined as FPG ≥ 126 mg/dl (≥7 mmol/L) or a random plasma glucose ≥ 200 mg/dl (≥11.1 mmol/L) in a patient with classic symptoms of hyperglycemia or hyperglycemic crisis, if a two hrs plasma glucose after oGTT was ≥ 200 mg/dl (≥11.1mmol/L), or HbA1c ≥6.5%, or specific treatments of a previously diagnosed diabetes mellitus. Insulin resistance was diagnosed if the HOMA-IR score was ≥ 2.5.

Metabolic syndrome (MS) was assessed in line with IDF criteria.

Hormonal assessment

Hypothalamic–pituitary–adrenal axis function was assessed by evaluating morning plasma ACTH, serum cortisol levels, aldosterone and renin by commercially available kits.

Cortisol circadian rhythm was explored by collecting cortisol blood samples every three hrs both at baseline and 12 months after the switch to OD-DR-HC.

Selected time points were: T0: 7am; T3hrs: 10 am; T6hrs: 1 pm; T9hrs: 4 pm; T12hrs: 7 pm; T15hrs: 10 pm; T18hrs: 1 am; T21hrs: 4 am; T24hrs: 7 am). First and last samples were collected before treatments.

The serum cortisol area under the curve (AUC) was calculated with the trapezoidal rule. Ten time slots were separately analyzed: AUC1: (7 am- 10 am); AUC2: (7 am- 1pm); AUC3: (1 pm- 7 pm); AUC 4: (7 pm- 1 am); AUC5: (1 pm- 1 am); AUC6: (1 am- 7 am); AUC7: (7 am- 7 pm); AUC8: (7 pm- 7 am); AUC9: (10 pm – 4 am); AUC10: (7 am- 7 am).

Quality of life assessment

Patients were asked to complete the updated Addison's disease-specific questionnaire (AddiQoL) a validated questionnaire used for QoL assessment in patients with AI. The questionnaire is composed by 30 questions. The response for each positive question was scored 1 (never/absolutely false), 2 (almost never/false and sometimes/partly false), 3 (more than half the days/ partly true and almost always/true), 4 (always/ absolutely true). The response for each negative question was scored 4 (never/ absolutely false), 3 (almost never/false and sometimes/partly false), 2 (more than half the days/partly true and almost always/true), 1 (always/absolutely true). Individual scores on the AddiQoL questionnaire can range from 30 to 120. The algebraic sum of points was calculated with higher scores indicating a higher level of health related QoL.

Depression assessment

Patients were asked to complete the Beck Depression Inventory II (BDI-II), a validated questionnaire used for depression status assessment. The questionnaire is composed by 21 questions. The response for each question was scored from 0 to 3. The algebraic sum of points was calculated to reach a total score ranging from 0 to 63: a total score of 0–13

indicated minimal depression, 14–19 mild depression, 20–28 moderate depression and 29–63 severe depression.

Safety assessment

Adverse Events (AEs) were graded, according to Common Terminology Criteria for adverse events (CT-CAE) version 3, on the basis of severity in grade 1 (mild), 2 (moderate), 3 (severe) and 4 (very severe, life-threatening or disabling). The patients kept a diary to document extra doses of OD-DR-HC and reasons they were taken. All interventions performed for the AEs management were carefully registered during the entire period of the study in all patients included in the study.

Outcomes

The current study aimed at investigating the impact of the switch from twice or thrice daily conventional GCs to OD-DR-HC in a cohort of 14 adult patients with AI.

Primary outcomes were changes from baseline to 12 months in the hormonal profile and particularly in the serum cortisol AUC 7 pm-1 am and 7 pm-7 am.

Secondary outcomes were changes from baseline and 12 months in the metabolic profile, assessed by measurement of BW, BMI, WC, SBP and DBP, lipid and glucose profile, in QoL, and in depression status. The safety profile evaluation represented another secondary endpoint of the study.

Statistical analysis

Data were analyzed using SPSS Software for Windows, version 20.0 (SPSS, Inc., Cary, NC package). Data are reported as Mean ± SD or as percentages. The comparison between the numerical data before and after treatment was made by non-parametric

Wilcoxon's test. The comparison between prevalences was performed by $\chi 2$ test. A two-sided p value of less than 0.05 was considered significant.

The evaluation of the AEs was performed for the entire period of treatment.

Results

Twelve months after the switch to OD-DR-HC, a significant decrease was observed in WC (p=0.004) **(Figure 10)**, whereas no significant changes were observed in BW, BMI, blood pressure and lipid profile.

Analysing glucose metabolism, 12 months after the switch to OD-DR-HC, a significant decrease was observed in both AUC for glucose and insulin (p=0.014 and p<0.05) **(Figure 11A and Figure 11B),** in insulin levels 2hrs after OGTT (p<0.05) **(Figure 12),** as well as a significant increase in ISI0' (p=0.032) **(Figure 13).** No significant changes were observed in fasting glucose and fasting insulin, HbA1c, HOMA index, Matsuda index, and ISI 120'.

No significant differences were observed in the prevalence of metabolic co-morbidities.

However, visceral obesity was observed in 13 (92.8%) patients at study entry and in 12 (85.7%) patients 12 months after OD-DR-HC, and insulin resistance was observed in four (28.6%) patients at baseline and in two (14.3%) patients 12 months after the switch to OD-DR-HC.

Analysing hormonal profile, no significant differences were reported in morning plasma ACTH, serum cortisol levels, aldosterone and renin. Exploring the cortisol circadian rhythm, 12 months after the switch to OD-DR-HC, a significant decrease was observed in serum cortisol levels at 7 pm (p=0.02) and 10 pm (p=0.029) (**Figure 14**), and particularly in AUC4 (7 pm- 1 am) (p=0.007) (**Figure 15A**) and AUC8 (7 pm- 7 am) (p=0.035) (**Figure 15B**).

No significant changes were found in AddiQoL scores and depression status 12 months after the switch to OD-DR-HC. No significant differences were observed in the prevalence of minimal, mild, moderate and severe depression.

OD-DR-HC treatment was generally safely conducted and well tolerated.

Short-term AEs, such as fatigue and asthenia, known to occur in the first eight weeks of treatment, spontaneously resolved. Particularly, during the first eight weeks of treatment, two patients (14.3%) reported mild asthenia. During the study, four patients (28.6%) received stress dosing, for fever in two cases, a mild acute viral illness of short duration in one case, and for a mild episode of gastroenteritis in the other.

No moderate, severe and very severe AEs, hospitalizations and deaths occurred during the study.

5. EX VIVO STUDY

Study design

A 24-week, randomised, active comparator, non-intervention, parallel-group, controlled, clinical trial was conducted at the Department of Experimental Medicine, Sapienza University of Rome in collaboration with the Department of Clinical Medicine and Surgery, Federico II University of Naples.

This study was approved by the ethics review board at Sapienza University of Rome and done in accordance with the Declaration of Helsinki and Good Clinical Practice.

Participants

Eligible patients were aged 18–80 years, had primary or secondary AI, were taking conventional GC therapy, consisting in cortisone acetate or IR-HC two or three times a day plus daily doses of fludrocortisone as needed, had been stable for at least 3 months before enrolment, and were willing to change their regimen according to random allocation.

An age-matched and sex-matched parallel group of healthy volunteers, named non-intervention control group, who were adrenally sufficient, recruited in a 1:4 ratio to patients with AI, was followed during the same period.

All patients provided written informed consent before entering the study, with respect to study participation, and confidentiality statement of data collection according to the Italian privacy policy. All data were anonymised.

Patients with AI were randomly assigned (1:1) to continue multiple daily doses of conventional GCs (standard treatment group) or to switch to OD-DR-HC tablet (switch treatment group) with a computer-generated random sequence. Randomisation was stratified by AI type (primary vs secondary) and BMI (<26.5 kg/m^2 vs 26.5–30 kg/m^2 vs >30 kg/m^2). Outcome assessors (independent) were masked to treatment allocation, and the

success of masking was tested by questioning. Patients were not masked to treatment allocation.

One hundred thirty-eight individuals were screened for eligibility, including 110 patients with AI and 28 healthy volunteers. Overall, 89 patients with AI were randomly assigned to the standard treatment group (n=43) or to the switch treatment group (n=46).

All 89 patients were included in the primary analysis. Twenty-five healthy volunteers were assigned to the non-intervention control group. Of the 89 patients with AI, 44 had primary AI and 45 had secondary AI.

Eleven (12%) of 89 patients with AI discontinued the study, eight of whom were receiving standard treatment. Reasons for dropout were patient's decision (n=7) and adverse events (n=4), including arthritis (n=1), presence of a mammary nodule requiring biopsy (n=1), and worsening of chronic kidney disease (n=2).

Study medication and dose adjustments

Patients assigned to continue standard therapy were instructed to take the first dose on waking before leaving their bed and subsequent doses according to their established schedule (two or three times a day), but with the last dose no later than 5 pm.

Patients allocated to OD-DR-HC were instructed to take the dose on waking, before leaving their bed.

For all participants, blood samples were collected in the morning, between 8 and 9 am, by research nurses after overnight fasting; participants had to take their usual morning dose 2 hrs before blood sampling.

Patients previously on multiple doses of IR-HC a day received the same total daily dose, whereas patients previously on cortisone acetate received 0.8 mg of HC per 1 mg of cortisone, as recommended by the European Medicines Agency drug fact sheet.

Intermediate doses were rounded up to the nearest 5 mg (eg, 22.5 mg to 25 mg) to avoid any potentially dangerous reduction in total daily dose.

All patients treated with fludrocortisone at study entry maintained their treatment also after the OD-DR-HC switch.

No change was allowed in any other medication or in GC dose or timing, except for in cases of intercurrent illnesses requiring upscaling of the dose (involved administration of IR-HC in both groups), and only after consultation with the study team.

Patients and controls were interviewed about their dietary habits and all were on a standard Mediterranean diet. General nutritional recommendations were provided.

Procedures

All investigations were performed by a central laboratory at Sapienza University of Rome.

Peripheral blood mononuclear cells (PBMCs) were isolated from fresh whole blood and gated. Briefly, the monocyte and lymphocyte gates were analysed for CD14 and CD16 expression to identify CD14+CD16- monocytes, CD14+CD16+ monocytes, and CD16+CD14- cells. Absolute cell counts were derived from the total cell counts provided by the haematological analyser (SYSMEX Roche, Indianapolis, IN, USA).

The lymphocyte gate was also analysed for CD3 and CD56 expression to identify CD56+CD3- natural killer cells, CD56-CD3+ T lymphocytes, and CD3+CD56+ cells. Natural killer cells were defined as CD14-CD19- CD3-CD56+ and re-analysed for CD16 expression to identify CD16+ natural killer cells. Natural killer cells were further divided into two subsets on the basis of CD56 density: CD56dim cells and CD56bright cells. B lymphocytes were quantified by analysis of CD19 expression in the lymphocyte gate.

The Human Fc Fragment of IgG Low Affinity IIIa Receptor ELISA Kit (MyBioSource, San Diego, CA, USA) was used to estimate the amount of soluble CD16 in the serum. The Human TACE ELISA Kit (ADAM17; Abcam, Cambridge, MA, USA) was used to estimate

the amount of disintegrin and metalloproteinase domain-containing protein 17 (ADAM17) in the serum.

Outcomes

The primary efficacy outcome was body weight change from baseline to 24 weeks. Secondary outcomes were changes from baseline to 12 and 24 weeks in metabolic profile, assessed by measurement of fasting blood glucose, insulin, HbA1c, BMI, waist circumference, and serum lipids and use of the HOMA index; immune profile, assessed by immunophenotyping of PBMCs and measurement of concentrations of soluble CD16 and ADAM17, full blood cell count, C-reactive protein, erythrocyte sedimentation rate, fibrinogen, and immunoglobulin; rate, duration, and severity of infections, assessed with an adaptation of the German National Cohort Questionnaire; and QoL, assessed with the updated Addison's disease-specific AddiQoL questionnaire.

Statistical analysis

Statistical analyses were performed with SPSS version 20.0 by a dedicated statistician - Service of Medical Statistics and Information Technology, Fatebenefratelli Foundation for Health Research and Education, Rome, Italy.

Assuming a standard deviation of 1.3 for body weight change (on the basis of published data) and 1 kg as the minimal clinically relevant difference between treatments, a sample size of 72 patients was estimated needed to provide 90% power to detect a 1 kg difference in the primary outcome, with a two-sided significance level of 0.05. In establishing the sample size, a possible drop out of the study of 20% of patients was considered.

Change from baseline was calculated as the value at 12 or 24 weeks minus the baseline value.

Efficacy analyses included data from all patients who had received at least one dose of study drug. Normality of distribution for all interventions at all time points was assessed using the Shapiro-Wilk's test ($p>0.05$). Log transformation or reciprocal transformation to correct for skewed data and a mixed-model analysis to assess changes in outcomes with accommodation for repeated measurements were used. In the mixed-model analysis, the patient was a random effect and treatment, time, and treatment-by-time interaction were fixed effects. The differences in change from baseline to week 12 and 24 between the groups were calculated using an ANCOVA model that included baseline outcome as a covariate and treatment as a fixed effect and used the last-observation-carried-forward principle. Other covariates were sex, BMI, age, smoking, type and duration of AI, diabetes, and white blood cell count.

Standardised residuals were tested for normality with Shapiro-Wilk's test. Homoscedasticity and homogeneity of variances were assessed by visual inspection and with Levene's test. Multicollinearity was assessed by calculation of the variance inflation factor. A calculation of least-squares mean estimates with 95% CIs of treatment differences between the groups was performed using Bonferroni correction. Subgroup analysis was done to report the significance of treatment-by-subgroup interaction. A two-sided p value of less than 0.05 was considered significant.

Discrete secondary endpoints were analysed using χ^2 analysis or Fisher's exact test in cases of few events. Odds ratios (ORs) and 95% CIs were calculated with a logistic regression model. Correlations between circulating protein concentrations and blood-cell subtypes using Pearson correlation were estimated.

Results

Baseline characteristics were similar for the two intervention groups, whereas the healthy volunteers in the control population had lower BMIs and lipid concentrations at baseline than did patients with AI.

Patients with AI had similar full blood counts to healthy volunteers, but higher T lymphocyte (CD3+) and B lymphocyte (CD19+) counts, higher numbers of classic pro-inflammatory monocytes (CD14+CD16–), and lower numbers of CD16+CD14– cells and CD16+ natural killer cells at baseline. Additionally, patients with AI had higher concentrations of soluble CD16 and ADAM17 at baseline than did healthy volunteers.

The total daily dose of GCs was well balanced between the intervention groups at randomisation and was not different between the groups at study end.

The mean body weight at 24 weeks was 72 kg (95% CI 67 to 78) in the switch treatment group and 71 kg (62 to 79) in the standard treatment group, which was a mean change from baseline of –2.1 kg (95% CI –4 to –0.3) in the switch treatment group and 1.9 kg (–0.1 to 3.9) in the standard treatment group. With adjustment for covariates, the estimated difference in mean body weight change between the two interventions at week 24 was –4 kg (–6.9 to –1.1; p=0.008).

Body weight reduction had a significant treatment-by-time interaction (p=0.001) in the switch treatment group, starting from week 12 and improving further at week 24, but not in the standard treatment group.

The estimated treatment difference between the intervention groups at week 24 was –1.7 kg/m² (95% CI –3 to –0.5; p=0.008) for BMI and –2.5 cm (95% CI –4.3 to –0.5; p=0.016) for waist circumference. The estimated treatment difference between the groups for HbA1c was –0.3% (95% CI –0.5 to –0.1; p=0.001) at week 24; no significant change was seen in

fasting blood glucose, insulin, or HOMA index among patients without diabetes, as well as in LDL cholesterol and triglycerides.

Numbers of classic pro-inflammatory monocytes (CD14+CD16–) were reduced at 12 and 24 weeks in the switch treatment group, with the baseline count almost reduced by 50% at week 24 (**Figure 16A**). The estimated treatment difference between the groups for CD14+CD16– monocytes was –351 cells per µL (95% CI –543 to –159; p=0.00054) from baseline to week 12 and –481 cells per µL (–701 to –261; p<0.0001) from baseline to week 24.

Conversely, the number of CD16+CD14– cells increased from baseline to week 12 and week 24 in the switch treatment group, but not in the standard treatment group, reaching a similar level to the control population (**Figure 16B**).

Although non-classic CD16+CD14+ monocyte counts were unaffected by treatment, the number of natural killer cells expressing CD16 increased from baseline to week 12 and week 24 in the switch treatment group.

Subgroup analysis revealed no treatment-by-subgroup interaction for any of the immune outcomes CD14+CD16– (p=0.563), CD16+CD14– (p=0.368), CD16+CD14+ (p=0.760), CD3–CD56+ natural killer cells (p=0.547), CD16+ natural killer cells (p=0.554), total infections score (IN1–IN5; p=0.737), flu or flu-like events (p=0.156), and AddiQoL total score (p=0.121).

A lag of about 8 weeks was observed before the effect of the treatment switch became detectable, excluding acute cell redistribution.

Concentrations of soluble CD16 and ADAM17 normalised at 12 weeks in the switch treatment group (**Figure 17**). The estimated treatment difference at 12 weeks was –0.26

ng/mL (95% CI –0.33 to –0.19; p<0.0001) for ADAM17 and –4.99 ng/mL (–6.21 to –3.74; p<0.0001) for soluble CD16.

The number of mild infections reported by patients allocated to the switch treatment group after 24 weeks of treatment was only slightly higher than the number reported by healthy volunteers. Similarly, the frequency of flu or flu-like events decreased from baseline to 24 weeks in the switch treatment group.

Post-hoc analyses showed significant associations between improvements in CD16+CD14– cell counts or infection scores and reductions in concentrations of soluble CD16 and ADAM17.

An increase in the AddiQoL score was observed at week 24 in the switch treatment group only, with an estimated treatment difference of 5 points (95% CI 1 to 9; p=0.027).

6. DISCUSSION

The *in vitro* part of the current study explores the effects of the exposure of HC, administered at concentrations inducing either non-physiological or physiological daily cortisol profiles, at different phases of the circadian rhythm, on insulin sensitivity, in an *in vitro* model of mouse skeletal muscle cell. In particular, the treatment with non-physiological HC concentration (TSC, inducing a circulating daily cortisol profile resembling that reached in AI patients treated with thrice-daily of conventional IR-HC with a steep cortisol profile), during bathyphase, the time-point of cell circadian rhythm corresponding to the early evening, is associated with an impairment of insulin sensitivity, which is not occurring during treatment with physiological HC concentrations TSB and TSA, which induce a circulating daily cortisol profile resembling that reached in AI patients treated with OD-MR-HC or in healthy subjects, respectively.

At molecular level, during bathyphase, compared to either TSB or TSA, TSC induced downregulation of the expression of several genes involved in the regulation of insulin sensitivity and, particularly, in the regulation of intracellular insulin receptor signaling and fatty acid metabolism, particularly fatty acid β-oxidation, whose impairment contributes to the development of insulin resistance. Conversely, non-physiological and physiological HC concentrations, during acrophase and midphase, the time-points of cell circadian rhythm corresponding to the early morning and the early afternoon, did not significantly affect insulin sensitivity, suggesting that GC exposure affects insulin sensitivity and consequently insulin-dependent glucose, lipid and protein metabolisms in a manner which is strictly associated with the cell circadian rhythm in skeletal muscle.

Insulin resistance is a clinical condition characterized by the inability of insulin to regulate the circulating levels of plasma glucose through the suppression of hepatic glucose

production and the stimulation of peripheral glucose utilization, especially in skeletal muscle; it is generally the consequence of a defect of insulin receptor signaling caused by downregulation of the expression, as well as gene mutations or post-transcriptional and/or post-translational modifications of insulin receptor and/or downstream effector molecules, mainly IRS-1 and IRS-2, which, in the skeletal muscle, are phosphorylated on the tyrosine or serine residues, therefore influencing positively or negatively, respectively, the intracellular transmission of the insulin signal. Persistent peripheral insulin resistance initially induces a compensative increase of insulin secretion by pancreatic β-cells, but lastly induces a gradual dysfunction and death of the pancreatic β-cells, triggering to the development of diabetes.

In addition to the impairment of glucose metabolism, an impairment of lipid metabolism also occurs, with the increase of circulating free fatty acids levels, induced by their excessive release from adipose tissue, and captured by skeletal muscle, where they accumulate into the cytoplasm of the cells, for the concomitant impairment of their mitochondrial β-oxidation, inducing a lipotoxic state due to lipid infiltration. The lipotoxic state is responsible for the exacerbation of the impairment of insulin receptor activity, directly and indirectly, through the induction of an inflammatory state, and it is secondary responsible for a decrease of amino acid incorporation protein synthesis, determining a catabolic state with predominance of protein degradation in skeletal muscle.

Several *in vitro* and *in vivo* studies in animal and/or human models have demonstrated that GCs directly regulate glucose, lipid and protein metabolisms, by different mechanisms, including the well-known interference with the insulin receptor signaling, with consequent impairment of insulin sensitivity and development of insulin resistance, which contributes not only to the development of an impairment of glucose tolerance, but also to the shift from muscle protein synthesis to muscle protein degradation and from anabolic to

catabolic state. These mechanisms are emphasized in condition of GC excess, including exogenous and endogenous CS, where skeletal muscle protein catabolism together with insulin resistance determines a progressive muscle atrophy and a systemic metabolic disorder.

Currently, little is known about the molecular mechanisms underlying the effect of GC excess, and particularly, the loss of the physiological cortisol circadian rhythm on the development of metabolic disorders, also due to the inexistence of specific models, although a role of the disruption of cell circadian clock and rhythm has been suggested. However, the specific role of non-physiological daily cortisol profile or circadian cortisol rhythm on the development of insulin resistance and the underlying molecular mechanisms, in the skeletal muscle, remains a major challenge.

The current study, for the first time, elucidated the metabolic effects of HC exposure, at different concentrations, in different time-points of the cell circadian rhythm by exploring the molecular mechanisms both at genomic and protein levels, in a synchronized *in vitro* model. In the current study, in order to determine the role of cell circadian rhythm in the HC-induced metabolic function, cell synchronization of the skeletal muscle cells C2C12 has been assessed by serum-shock protocol; this protocol efficiently induced the circadian expression of the main components of the clock machinery and allowed to fix the time-points of treatment with HC. Previous reports have found that the addition of serum-rich media to cultured mammalian cells triggers the rhythmic expression of cell circadian clock, given the largely demonstrated presence of cell autonomous circadian clock, regardless of their species of origin. In particular, as previously demonstrated in different *in vitro* models, despite the murine origin, in C2C12 cells, serum shock induced circadian clock rhythmic

expression, by resetting endogenous clock genes expression, and its reactivation in a circadian manner.

The rhythmic oscillation of clock genes through the 24 hrs period allowed to establish the circadian time-points of treatment, which, for the purpose of this study, have been set at Bmal1 acrophase, midphase and bathyphase, corresponding to maximum, medium and minimum expression levels, respectively. The circadian clock consists of an autoregulatory transcriptional/translational feedback loop mechanism with a positive and a negative arm; this mechanism predicts that the expression levels of Bmal1, the main effector of the loop mechanism positive arm, are at the highest levels in the first hrs of light and at the lowest levels in the first hrs of dark, with an opposed trend for Per and Cry expression levels, the main effectors of the loop mechanism negative arm, whose levels are highest in the first hrs of dark and lowest in the first hrs of light. Starting from these observations, 12 hrs after serum shock, high Bmal1 and low Per and Cry expression was observed, while 20 hrs after serum shock, a reversal trend was observed, as previously demonstrated in the same cell model. Assuming 12 hrs after serum shock as corresponding to the early morning, 15 hrs after serum shock corresponding to the early afternoon and 20 hrs after serum shock corresponding to the early evening, different treatment schedules of HC were selected, inducing different physiological or pathological circulating cortisol daily curves.

In particular, TSB and TSC, corresponding to HC concentrations used to mimic circulating cortisol concentrations reached in AI patients treated with OD-MR-HC and thrice-daily of conventional IR-HC, respectively, were compared to TSA, corresponding to HC concentrations used to mimic physiological circulating cortisol concentrations in healthy subjects, specifically at the different cell circadian rhythm time-points acrophase, midphase and bathyphase.

After the different treatment schedules, gene expression levels of 84 genes involved in the modulation of insulin sensitivity, and the development of insulin resistance, were evaluated

and compared through genomic array, to obtain a first evaluation of HC exposure genomic effects on skeletal muscle insulin sensitivity in the three different cell circadian time-points. In detail, TSB and TSC, when compared to TSA during acrophase and midphase, did not significantly influence expression levels of genes involved in the regulation of insulin sensitivity, despite the relatively high HC concentrations. Conversely, TSC, but not TSB, during bathyphase, induced a significant downregulation in the expression of 21 main genes involved in the regulation of insulin sensitivity, despite the relatively low concentrations of HC. An in-depth study of the function of these 21 genes showed their involvement in the regulation of intracellular insulin receptor signaling and a specific intracellular pathway of lipid metabolism, namely fatty acid β-oxidation. These interesting novel results demonstrated that the exposure of skeletal muscle cells to relatively low HC concentrations during the cell bathyphase, which typically occurs in the early evening of the physiological circadian rhythm, can strongly and negatively influence the intracellular transmission of insulin signal, disrupting the expression of the main genes involved in the regulation of insulin sensitivity, pointing out that the day-time, more than the degree, of HC exposure negatively influence insulin sensitivity in the skeletal muscle. Indeed, although the HC concentration used in TSC was only slightly higher than the HC concentrations used in TSB and TSA during bathyphase, a great number of genes involved in the regulation of insulin sensitivity was negatively regulated, whereas in acrophase and midphase, although the HC concentrations used in TSB and TSC were notably higher than the those used in TSA, no significant changes have been observed among the three different HC administration schedules, in the expression of genes involved in the regulation of insulin sensitivity, therefore emphasizing that the metabolic GC effects depend on the different phases of cell circadian rhythm, probably as a consequence of the effect of the circadian clock on the GC action, mediated by the change in GC receptor sensitivity.

Moreover, in the current study, to better investigate the involvement of the 21 genes significantly downregulated in skeletal muscle insulin resistance during bathyphase, the five genes mainly involved in the regulation of insulin sensitivity (Insr, Irs1, Irs2, Pi3kca and Adipor2) were selected and re-analyzed through RT-qPCR, confirming their decreased expression exclusively after TSC exposure, and that, rather than the HC doses, the specific time-point of the circadian rhythm, at which they are administered, is the major responsible of the disruption in the transmission of the insulin signal. The confirmation of the downregulation of these genes allowed to perform an additional molecular analysis, at protein level, to better investigate the intracellular insulin signal activation after the treatment schedules at cell bathyphase, the only time-point of the cell circadian rhythm with significantly relevant change in gene expression.

In detail, the analysis of intracellular proteins involved in the insulin receptor signaling and in the fatty acid β-oxidation pathway corroborated the results obtained at genomic level. Indeed, following the pathological TSC schedule, insulin signaling was weakened as demonstrated by the strong inhibition of phosphorylated IRS1 at Thyr608 (insulin receptor activating phosphorylation) and of phosphorylated AKT at Ser473 (intracellular insulin pathway activation), compared to insulin signaling activated by physiological TSA and TSB. Moreover, the concomitant inhibition of AMPKα phosphorylation at Thr172 and of ACC at Ser79 in TSC compared to TSB and TSA suggested that HC supra-physiological TSC during bathyphase might inhibit fatty acid β-oxidation, compared to physiological TSA and TSB.

The current *in vitro* study presents some limitations concerning the *in vitro* study of cell circadian rhythm. Although the oscillation of the clock genes is maintained at the peripheral level, in this *in vitro* system, the SCN input as well as the pharmacokinetics parameters regulating HC exposure *in vivo*, are missed. *In vivo* cortisol circulating levels and bioavailability are strongly affected by protein binding activity, metabolism and

excretion in urine among the individuals, making it impossible to predict in an *in vitro* system. However, although the concentrations of cortisol may vary between individuals the pattern of cortisol circadian rhythm is sufficiently reproducible. Moreover, the *in vitro* exposure to HC for only one hour in order to avoid the cell desynchronization and the loss of the Bmal1 acrophase, certainly did not allow to investigate the gene and protein modifications that would have occurred with a more prolonged treatment.

Despite these limitations, these current findings might support the clinical knowledge about cortisol circadian rhythm disruption and metabolic comorbidities.

Indeed, these preclinical evidences have already been confirmed in the *in vivo* part of the current study, conducted in patients suffering from AI, exposed to GCs administered at concentrations inducing either non-physiological or physiological daily cortisol profiles.

In a homogenous cohort of AI patients switched from conventional GCs to OD-DR-HC, a significant improvement has been observed in waist circumference and glucose metabolism, in terms of both area under the curve for glucose and insulin, in insulin levels 2hrs after glucose load, as well as in the fasting insulin sensitivity index.

Considering that the mean and median dose of conventional GCs and OD-DR-HC were similar, the results of the current study suggest that the improvement in waist circumference and insulin sensitivity of these patients is due to the more physiological daily cortisol profile of OD-DR-HC compared with conventional GCs, and in particular OD-DR-HC appeared able to adequately maintain cortisol replacement during the 24 hrs, with a significant decrease in serum cortisol levels in the early evening (7-10 pm) and during the night, from 7 pm to 1 am and from 7 pm to 7 am. This low cortisol exposure during the early evening and the night, should be considered to be important to prevent the evening cortisol overexposure. Indeed, it is well known that HC administered in the evening is associated with more pronounced detrimental effects and particularly insulin resistance,

visceral obesity, coronary artery calcification, impaired well-being and sleep quality. Therefore, this reduced night-time exposure to GCs may have a strong impact on disease management and health outcome.

AI patients maintained a mortality rate higher than that associated with the general population, together with a higher morbidity for metabolic disorders, as well as cardiovascular, infectious, immune and skeletal diseases, resulting in an impaired QoL. Historically the total daily dose reduction has been advocated to counteract the most deleterious effects of GC overtreatment, and the total GC exposure dose was considered responsible for the considerable morbidity and mortality reported in AI patients. However, most epidemiological studies have not shown an association between total daily GC dose and metabolic status.

More recently, a key role in determining morbidity of AI patients has been attributed to the disruption of GC circadian rhythmicity induced by the conventional GC formulations. Indeed, the most commonly used conventional IR-HC thrice daily treatment schedule is associated with a non-physiological cortisol daily pattern, not providing an adequate GC physiological replacement therapy, mainly due to the high circulating cortisol levels in the evening. Consistently, primary and secondary AI patients treated with thrice daily conventional formulations, especially IR-HC, and exposed to the non-physiological cortisol pattern, when switched to OD-MR-HC therapy, able to better mimic the circadian cortisol profile, reducing the exposure in the afternoon and evening, showed improvements in metabolic parameters, including body weight, waist circumference, lipid profile and, particularly, in glucose metabolism, with reduction in fasting glucose and glycated hemoglobin in diabetic patients, reduction in insulin levels and insulin resistance in pre-

diabetic patients, and a reduction in fasting glucose, glycated hemoglobin, insulin levels and insulin resistance in non-diabetic patients.

Beyond efficacy, in the current study OD-DR-HC was demonstrated able to maintain a good safety profile, during the 12 consecutive months of therapy. According to the largest and longest prospective trial evaluating the safety of OD-DR-HC in AI patients, this study showed that long-term maintenance OD-DR-HC treatment was well tolerated. The increased incidence of fatigue and asthenia reported during the first eight weeks of treatment, may reflect on one hand the higher vigilance of both patients and clinicians to monitor AEs while receiving therapy in the context of a clinical trial, and on the other hand, the potential psychological impact of changing an established conventional treatment regimen.

The optimal outcome in the management of the intercurrent illness episodes, such as fever, a mild acute viral illness and a mild episode of gastroenteritis, reported in less than 30% of patients, suggested that OD-DR-HC is at least as effective as conventional GC therapy in controlling intercurrent illnesses. The absence of moderate, severe and very severe AEs, hospitalizations and deaths of patients receiving OD-DR-HC, confirmed its very safe profile.

Obviously, this *in vivo* study presents some limitations: first, it has an open-label, non-randomized, non-controlled study, in which patients decided whether they wanted to change to OD-DR-HC or to stay on conventional GCs, being not blinded to treatment and probably their expectations on the efficacy of the new drug could have, at least partially, affected results. Secondly, the small number of patients, due to the rarity of the disease may not allow definitive conclusions. Therefore, a case-control, cross-over study,

performed in a larger cohort of patients, with a longer follow-up period, is needed to verify and confirm these preliminary results.

Despite these limitations, this study has important strengths: it is the first study assessing the effects of OD-DR-HC on cortisol circadian rhythm through the 24 hrs in a homogeneous cohort of AI patients after a long period of 12 months of treatment, representing a single tertiary care Italian centre experience, with a great similarity to common clinical practice.

The last part of the current study, conducted collaborating with the Sapienza University of Rome, tried to mainly investigate and better detail the interplay between GC therapy, administered at concentrations inducing either non-physiological or physiological daily cortisol profiles, and immune system. Indeed, the immune system, which is highly sensitive to GCs, has seldom been investigated in AI patients receiving lifelong GC replacement therapy. The immunosuppressive effects of high doses of GCs are known. However, the subtle long-term changes occurring with multiple daily doses of low amounts of GCs are largely unknown and no previous studies have investigated changes to the immune system in patients with primary or secondary AI switching from multiple doses a day to a OD-DR-HC.

Compared with a control population, patients with AI on conventional replacement GC therapy had unexpected abnormalities in circulating PBMCs, which were not evident on a routine full blood count. An increased number of classic monocytes and a reduced number of CD16+ natural killer cells were found at baseline in AI patients, which reversed after switching from the multi-dose regimen to the once-daily regimen. Consequently, the frequency of infections, mainly the number of recurrent upper respiratory tract infections, appeared reduced in patients who switched to once-daily administration.

Historically, the susceptibility of AI patients to infections has been attributed to the immunosuppressive effects of high doses of GCs, despite patients often being treated with low doses of GCs. However, more recently AI patients receiving HC replacement therapy three times a day reported selective impairment of natural killer cell cytotoxicity.

Natural killer cells provide innate defence against virally infected and transformed cells, but also participate in immune regulation. Through the CD16 receptor, natural killer cells can activate antibody-dependent cell-mediated cytotoxicity and, hence, interface with adaptive immunity.

The significant depletion of CD16+ natural killer cells observed in AI patients in the current study impairs activation of antibody-dependent cell-mediated cytotoxicity by natural killer cells, thus favouring infections. Particularly, patients with AI on conventional GC therapy had an increased number of classic monocytes (CD14+CD16–). Switching from multiple to OD-DR-HC reduced CD14+CD16– counts and restored counts of CD16+CD14– cells and CD16+ natural killer cells. To investigate whether the Fc receptor was lost or simply not expressed, the soluble form of CD16 was measured. The soluble CD16 concentration was elevated in patients with AI compared with controls and normalised after patients switched to the once-daily regimen.

Therefore the results of the current study suggest that desynchronisation of the clock can affect immune function, and that one of the most important factors causing hospital admission in AI patients, consisting in recurrent infections and mainly respiratory and gastrointestinal tract infections, can be managed by changing the circadian timing of GC administration. Mimicking a more circadian rhythm also improved body weight and QoL in AI patients treated with OD-DR-HC compared with conventional GC regimens.

Lastly, also in this multicentre experience transition to OD-DR-HC appeared to be safe, with no significant differences in frequency or severity of AEs between the two treatment groups.

This multicentre study has several advantages, including the sample size, random allocation, masking of the assessor, duration, and inclusion of a control group. However, this multicentre study presents some limitations: first, participants were not masked to treatment allocation, risking recollection bias; secondly, a self-reported questionnaire was used to measure infection rates. Lastly, a 24 hrs sampling was not performed to investigate correlations with the different pharmacokinetics of the two GC regimens.

In conclusion, OD-DR-HC, better mimicking the cortisol circadian rhythm, improved metabolic and immune functions of AI patients compared with conventional multiple daily GC doses. In AI patients with poor metabolic control, recurrent infections and impaired QoL, a replacement GC therapy which better mimics the circadian rhythm of endogenous cortisol may offer measurable benefits.

7. POSSIBLE APPLICATION POTENTIALITIES

The current study aims to synergistically improve understanding the impact of GC circadian rhythm disruption on metabolic and immune systems, in patients with AI, characterizing the correlated pathophysiological mechanisms and clinical complications involved in the increased risk of morbidity and QoL impairment.

These results might potentially also be useful to the recognition and management of large categories of subjects with GC circadian disruption, such as subjects exposed to high exogenous GC doses for systemic diseases, or to chronic stress, and shift workers, therefore holding a relevant impact on public health.

The study addresses relevant issues in metabolic and immune pathways related to GC circadian rhythm disruption, impacting on AI patient's management.

Deeper understanding of how the clock system mediates the control over muscle tissue might offer novel strategies against metabolic disorders, including metabolic syndrome, diabetes, dyslipidaemia and obesity.

The other part of the study addresses relevant issues in immune pathway related to GC circadian rhythm disruption, impacting on AI patient's management, offering novel strategies against immune disorders and infectious diseases.

Addressing these relevant issues might improve QoL, reduce mortality risk as well as total costs for health, in terms of medications, hospitalization and loss of workdays.

Challenging goals are to select the best AI patient candidate to receive a more physiologic GC treatment; to obtain a better tailored GC replacement treatment in AI patients, greatly improving their QoL and potentially reducing their morbidity and mortality.

The main impacts are to reduce morbidity, mortality and to improve QoL in patients with AI, and potentially in subjects exposed to high GC doses for systemic diseases, to chronic stress, and shift workers; to contribute in elucidating the role of GC circadian rhythm disruption in muscle tissue pathway, with results which would be relevant for the treatment of metabolic disorders, for which there is still considerable unmet medical need; to contribute in elucidating the role of GC circadian rhythm disruption in immune cells and clock-related gene expression, by allowing to develop novel tools to measure the GCs impact on immune function in humans, with results which would be relevant for the prevention of infectious diseases and sepsis; to gain insights into the treatment of AI, by developing strategies of tailored therapies with preventive and therapeutic implications in a novel challenging field of chrono-pharmacology; to provide chrono-therapeutic interventions, optimizing drug effects and/or minimizing toxicity by timing medications with regard to biological rhythms; to improve the understanding of circadian and thus, predictable, changes in pharmacological desired effects (chrono-effectiveness) and tolerance (chrono-tolerance) in the era of tailor medicine.

The results of the current study are novel and original, and may provide relevant advancement in both the clinical and pharmaceutical fields, by opening novel areas of investigation and therapeutic applicative potentials, and by filling the growing need for tailored treatment approach, in order to achieve challenging treatment goals.

Obviously, whether the observed effects of the timing of GC administration could be transferred outside AI deserves further studies.

8. REFERENCES

- Alberti KG Et al. IDF Epidemiology Task Force Consensus Group. The metabolic syndrome a new worldwide definition. Lancet 2005
- Al-Shoumer KAS et al. Effect of glucocorticoid replacement therapy on glucose tolerance and intermediary metabolites in hypopituitary adults. Clin Endocrinol (Oxf). 1995
- American Diabetes Association. Classification and diagnosis of diabetes. In Standards of Medical Care in Diabetes 2020. Diabetes Care 2020
- Ando H et al. Clock gene expression in peripheral leucocytes of patients with type 2 diabetes. Diabetologia 2009
- Aoyagi T et al. Characteristics of circadian gene expression in mice white adipose tissue and 3T3-L1 adipocytes. Journal of Health Science 2005
- Balsalobre A et al. A serum shock induces circadian gene expression in mammalian tissue culture cells. Cell 1998
- Barnea M et al. Dexamethasone induces high-amplitude rhythms in preadipocytes, But hinders circadian expression in differentiated adipocytes. Chronobiol Int. 2013
- Beck et al. Comparison of Beck Depression Inventories -IA and -II in psychiatric outpatients. J Pers Assess. 1996)
- Bensing S et al. Increased death risk and altered cancer incidence pattern in patients with isolated or combined autoimmune primary adrenocortical insufficiency. Clin Endocrinol (Oxf). 2008
- Bergthorsdottir R et al. Premature mortality in patients with Addison's disease: A population-based study. J Clin Endocrinol Metab. 2006
- Bornstein SR et al. Diagnosis and Treatment of Primary Adrenal Insufficiency: An Endocrine Society Clinical Practice Guideline JCEM 2016
- Buckingham JC. Glucocorticoids: Exemplars of multi-tasking. Br J Pharmacol. 2006

- Castell S et al. Test-retest reliability of an infectious disease questionnaire and evaluation of self-assessed vulnerability to infections: findings of Pretest 2 of the German National Cohort. Bundesgesundheitsblatt Gesundheitsforschung Gesundheitsschutz 2014
- Chan S and Debono M Replication of cortisol circadian rhythm: new advances in hydrocortisone replacement therapy. Ther Adv Endocr Metab 2010
- Cheng HY et al. microRNA modulation of circadian-clock period and entrainment. Neuron 2007
- Crowley RK et al. Central hypoadrenalism JCEM 2014
- Cuesta M et al. Simulated Night Shift Disrupts Circadian Rhythms of Immune Functions in Humans. J Immunol 2016
- Curtis AM et al. Circadian clock proteins and immunity. Immunity 2014
- Danilowicz K et al. Correction of cortisol overreplacement ameliorates morbidities in patients with hypopituitarism: A pilot study. Pituitary. 2008
- Debono M et al. Novel strategies for hydrocortisone replacement. Best Pract Res Clin Endocrinol Metab. 2009
- De Bruyne JP et al. A Clock Shock: Mouse CLOCK Is Not Required for Circadian Oscillator Function. Neuron. 2006
- De Kloet ER et al. Brain corticosteroid receptor balance in health and disease. Endocr Rev. 1998
- Dunlop D Eighty-Six Cases of Addison's Disease. British medical journal 1963
- European Medicines Agency. Annex I. Summary of product characteristics. http://www.ema.europa.eu/docs/en_GB/document_library/EPAR__Product_Information/human/002185/ WC500117637.pdf (accessed Oct 7, 2017)
- Filipsson H et al. The impact of glucocorticoid replacement regimens on metabolic outcome and comorbidity in hypopituitary patients. J Clin Endocrinol Metab. 2006

- Fleseriu M et al. Hormonal replacement in hypopituitarism in adults: An endocrine society clinical practice guideline. J Clin Endocrinol Metab. 2016
- Frara S et al. Bone safety of dual-release hydrocortisone in patients with hypopituitarism. Endocrine. 2018
- Fu L, Lee CC. The circadian clock: Pacemaker and tumour suppressor. Nat Rev Cancer. 2003
- Gamble KL et al. Circadian clock control of endocrine factors. Nature reviews Endocrinology 2014
- Gangwisch JE Epidemiological evidence for the links between sleep, circadian rhythms and metabolism. Obes Rev 2009
- García-Borreguero D et al. Glucocorticoid replacement is permissive for rapid eye movement sleep and sleep consolidation in patients with adrenal insufficiency. J Clin Endocrinol Metab. 2000
- Gathercole LL et al. Glucocorticoid modulation of insulin signaling in human subcutaneous adipose tissue. J Clin Endocrinol Metab. 2007
- Giordano R et al. Improvement of anthropometric and metabolic parameters, and quality of life following treatment with dual-release hydrocortisone in patients with Addison's disease. Endocrine. 2016
- Gómez-Abellán P et al. Glucocorticoids Affect 24 h Clock Genes Expression in Human Adipose Tissue Explant Cultures. PLoS One. 2012
- Gómez-Santos C et al. Circadian rhythm of clock genes in human adipose explants. Obesity 2009
- Guarnotta V et al. Improved insulin sensitivity and secretion in prediabetic patients with adrenal insufficiency on dual-release hydrocortisone treatment: a 36-month retrospective analysis. Clin Endocrinol (Oxf). 2018

- Guarnotta V et al. Dual-release hydrocortisone improves hepatic steatosis in patients with secondary adrenal insufficiency: A real-life study. Ther Adv Endocrinol Metab. 2019
- Guarnotta V et al. Dual-release hydrocortisone vs conventional glucocorticoids in adrenal insufficiency. Endocr Connect. 2019
- Heegaard NH et al. Diurnal Variations of Human Circulating Cell-Free Micro-RNA. PlosOne 2016
- Hindmarsh PC & Charmandari E Variation in absorption and half-life of hydrocortisone influence plasma cortisol concentrations. Clinical endocrinology 2015
- Hurley MJ et al. Circadian Oscillators: Around the Transcription-Translation Feedback Loop and on to Output. Trends Biochem Sci 2016
- Hu Z at al. Endogenous glucocorticoids and impaired insulin signaling are both required to stimulate muscle wasting under pathophysiological conditions in mice. J Clin Invest. 2009
- Isidori AM et al. Effect of once-daily, modified-release hydrocortisone versus standard glucocorticoid therapy on metabolism and innate immunity in patients with adrenal insufficiency (DREAM): a single-blind, randomised controlled trial. Lancet Diabetes Endocrinol 2018
- Jiang CL et al Why do we need nongenomic glucocorticoid mechanisms? Front Neuroendocrinol. 2014
- Johannsson G et al. Improved cortisol exposure-time profile and outcome in patients with adrenal insufficiency: a prospective randomized trial of a novel hydrocortisone dual-release formulation. JCEM 2012
- Kelly MA et al. Circadian gene variants and susceptibility to type 2 diabetes: A pilot study. PLoS One. 2012

- Kim TW et al. The impact of sleep and circadian disturbance on hormones and metabolism. International journal of endocrinology 2015
- Landgraf D et al. NPAS2 Compensates for Loss of CLOCK in Peripheral Circadian Oscillators. PLoS Genet. 2016
- Lee P et al. Brown adipose tissue exhibits a glucose-responsive thermogenic biorhythm in humans. Cell Metabolism 2016
- Leliavski A et al. Adrenal clocks and the role of adrenal hormones in the regulation of circadian physiology. Journal of biological rhythms 2015
- Mah PM et al. Weight-related dosing, timing and monitoring hydrocortisone replacement therapy in patients with adrenal insufficiency. Clin Endocrinol. 2004
- Matthews KA et al. Positive and negative attributes and risk for coronary and aortic calcification in healthy women. Psychosom Med 2006
- Matthews DR et al. Homeostasis model assessment: insulin resistance and beta-cell function from fasting plasma glucose and insulin concentrations in man. Diabetologia 1985
- Mazzoccoli G et al. Clock Genes and Clock-Controlled Genes in the Regulation of Metabolic Rhythms. Chronobiology Int 2012
- Mezzullo M et al. Validation of an LC-MS/MS salivary assay for glucocorticoid status assessment: Evaluation of the diurnal fluctuation of cortisol and cortisone and of their association within and between serum and saliva. J Steroid Biochem Mol Biol 2016
- Mongioì LM et al. Dual-release hydrocortisone treatment: Glycometabolic profile and health-related quality of life. Endocr Connect. 2018
- Morgan SA et al. 11β-hydroxysteroid dehydrogenase type 1 regulates glucocorticoid- induced insulin resistance in skeletal muscle. Diabetes. 2009

- Nader N et al. Interactions of the circadian CLOCK system and the HPA axis. Trends Endocr Metab 2010
- National Cholesterol Education Program (NCEP) Expert Panel on Detection, Evaluation, and Treatment of High Blood Cholesterol in Adults (Adult Treatment Panel III). Third Report of the National Cholesterol Education Program (NCEP) Expert Panel on Detection, Evaluation, and Treatment of High Blood Cholesterol in Adults (Adult Treatment Panel III) final report. Circulation. 2002
- National Cancer Institute Common terminology criteria for adverse events v3.0(CTCAE) 2006 Availableat:http://ctep.cancer.gov/protocolDevelopment/electronic_applications/docs/ctcaev3.pdf
- Nicod N et al. Metabolic adaptations to dexamethasone-induced insulin resistance in healthy volunteers. Obes Res. 2003
- Nielsen MF et al. Impaired basal glucose effectiveness but unaltered fasting glucose release and gluconeogenesis during short-term hypercortisolemia in healthy subjects. Am J Physiol - Endocrinol Metab. 2004
- Nilsson AG et al. Long-term safety of once-daily, dual-release hydrocortisone in patients with adrenal insufficiency: a phase 3b, open-label, extension study. Eur J Endocrinol. 2017
- Ninel Hansen S et al. Keeping fat on time: Circadian control of adipose tissue. Exp Cell Res 2017
- Oksnes M et al. Quality of life in European patients with Addison’s disease: validity of the disease-specific questionnaire AddiQoL. J Clin Endocrinol Metab 2012
- Otway DT et al. Circadian rhythmicity in murine pre-adipocyte and adipocyte cells. Chronobiol Int 2009

- Partch CL et al. Molecular architecture of the mammalian circadian clock. Trends in cell biology 2014
- Peter HH et al. Construction and clinical validation of a questionnaire-based risk score to identify patients suffering from immunodeficiency or systemic autoimmunity. Br J Med Med Res 2014
- Pivonello C et al. Effects of the single and combined treatment with dopamine agonist, somatostatin analog and mTOR inhibitors in a human lung carcinoid cell line: an in vitro study. Endocrine. 2017
- Pivonello R et al. Complications of Cushing's syndrome: state of the art. Lancet Diabetes Endocrinol 2016
- Plat L et al. Metabolic effects of short-term elevations of plasma cortisol are more pronounced in the evening than in the morning. JCEM 1999
- Quinkler M et al. Modified-release hydrocortisone decreases BMI and HbA1c in patients with primary and secondary adrenal insufficiency. Eur J Endocrinol 2015
- Schroeder AM, Colwell CS. How to fix a broken clock. Trends Pharmacol Sci 2013
- Shang Z et al. Effect of HS on the circadian rhythm of mouse hepatocytes. Lipids Health Dis 2012
- Sievers C et al. Evaluation of a questionnaire to assess selected infectious diseases and their risk factors: findings of a multicenter study. Bundesgesundheitsblatt Gesundheitsforschung Gesundheitsschutz 2014
- Somanath PR et al. Deficiency in core circadian protein Bmal1 is associated with a prothrombotic and vascular phenotype. J Cell Physiol 2011
- Tappy L et al. Mechanisms of dexamethasone-induced insulin resistance in healthy humans. J Clin Endocrinol Metab. 1994
- Tsang AH et al. Rodent Models for the Analysis of Tissue Clock Function in Metabolic Rhythms Research Front Endocrinol 2017

- Tsoumtsa LL et al. Circadian Control of Antibacterial Immunity: Findings from Animal Models. Front Cell Infect Microbiol 2016
- Turek FW et al. Obesity and metabolic syndrome in circadian Clock mutant nice. Science (80-). 2005
- Vgontzas AN et al. Chronic insomnia is associated with nyctohemeral activation of the hypothalamic-pituitary-adrenal axis: clinical implications. J Clin Endocrinol Metab. 2001
- Vieira E et al. Altered clock gene expression in obese visceral adipose tissue is associated with metabolic syndrome. PlosOne 2014
- Viswambharan H et al. Mutation of the circadian clock gene Per2 alters vascular endothelial function. Circulation 2007
- Weber MA et al. Clinical practice guideline for the management of hypertension in the community: a statement by the American Society of Hypertension and the International Society of Hypertension. J Clin Hypertens. 2014
- Wefers J et al. Circadian misalignment induces fatty acid metabolism gene profiles and compromises insulin sensitivity in human skeletal muscle. Proc Natl Acad Sci U S A. 2018
- Xiang S et al. Oscillation of clock and clock controlled genes induced by serum shock in human breast epithelial and breast cancer cells: Regulation by melatonin. Breast Cancer Basic Clin Res. 2012
- Yaffe D et al. Serial passaging and differentiation of myogenic cells isolated from dystrophic mouse muscle. Nature, 1977
- Yang G et al. Timing of expression of the core clock gene Bmal1 influences its effects on aging and survival. Sci Transl Med 2016
- Yang S et al. The role of mPer2 clock gene in glucocorticoid and feeding rhythms. Endocrinology. 2009

- Yaribeygi H et al. Insulin resistance: Review of the underlying molecular mechanisms. J Cell Physiol. 2019
- Yuan L et al. Chronobiology 2017 Nobel Prize in Physiology or Medicine Yi Chuan 2018
- Ye R et al. Dual modes of CLOCK:BMAL1 inhibition mediated by Cryptochrome and period proteins in the mammalian circadian clock. Genes Dev. 2014

9. FIGURES & TABLES

Figure 1. Simplified representation of the in vitro synchronization protocol

C2C12 myoblasts were seeded in 60 mm dishes and terminally differentiated to myocytes. After 48 hrs, the medium was changed and C2C12 were synchronized using DMEM-supplemented with 50% horse serum HS (serum shock). After 2 hrs in serum-rich medium, cells were rinsed and re-fed with serum-free DMEM for 24 hrs.

Figure 2. Simplified representation of TSA and TSC performed in the different circadian time-points

At the indicated times (every 4 hrs over a 24 hrs period) dishes were washed twice with ice-cold PBS 1X, lysed, and RNA extracted from cell lysates. At each time-point of the cell circadian cycle, corresponding to 8 am, 1 pm and 6 pm of the subjective daily rhythm, C2C12 cells were exposed to different HC concentrations for 1h.

Figure 3. Circadian messenger and protein expression profile of Bmal1, Clock, Per1, Per2 and Cry2 in C2C12 cell line

A) Double plotted graphs illustrating the temporal rhythm organization of *Bmal1, Clock, Per1, Per2* and *Cry2* in synchronized C2C12 cell line during 24 hrs. The messenger expression levels were normalized against the housekeeping gene *Rna18s*. Values represent the mean ± SEM of six independent experiments. P values depicted in each graph were calculated by ANOVA. B) Protein expression profile of BMAL1, PER1, PER2 and CRY2 during 24 hrs. Proteins were normalized against b-ACTIN. The blot is representative of two or three independent experiments.

Figure 4. Volcano plot representation indicates the statistical significance of gene expression changes comparing the exposure to several HC concentrations at acrophase time point of circadian rhythm

Comparison between TSA vs TSB (A). Comparison between TSA vs TSC (B). Comparison between TSB vs TSC (C). The x-axis of the Volcano plot shows the log2 of the fold-differences, while the y-axis their p-values based on student's t-test. Symbols in the volcano plot above the dashed line readily identify fold-differences. The plot represents the mean of three independent experiments.

Figure 5. Volcano plot representation indicates the statistical significance of gene expression changes comparing the exposure to several HC concentrations at midphase time point of circadian rhythm

Comparison between TSA vs TSB (A). Comparison between TSA vs TSC (B). Comparison between TSB vs TSC (C). The x-axis of the Volcano plot shows the log2 of the fold-differences, while the y-axis their p-values based on student's t-test. Symbols in the volcano plot above the dashed line readily identify fold-differences. The plot represents the mean of three independent experiments.

Figure 6. Volcano plot representation indicates the statistical significance of gene expression changes comparing the exposure to several HC concentrations at bathyphase time point of circadian rhythm

Comparison between TSA vs TSB (A). Comparison between TSA vs TSC (B). Comparison between TSB vs TSC (C). The x-axis of the Volcano plot shows the log2 of the fold-differences, while the y-axis their p-values based on student's t-test. Features of interest are typically those in the upper left and right hands corners of the volcano plot, as these have large fold changes (lie far from x=0) and are statistically significant (have large y-

values). (www.qiagenbioinformatics.com). Plots circled in red indicate significantly modified genes. The plot represents the mean of three independent experiments.

Figure 7. Insulin pathway genes validation through RT-qPCR

Values represent the mean ± SEM of three independent experiments. The expression levels are normalized against the housekeeping gene cyclophilin. **p<0.01; ***p<0.001 vs control

Figure 8. Intracellular insulin signaling after different HC concentrations at bathyphase time point

The blots are representative of three independent experiments. The values of densitometry reported are the mean ± SEM of three independent experiments.

Figure 9. Schematic representation of intracellular insulin signaling and fatty acid ß oxidation pathway activated by TSC in bathyphase of Bmal1 (Created with BioRender.com).

Exposure of muscle cells to TSC in bathyphase strongly inhibits pIRS-1 Tyr608, thus decreasing intracellular insulin signaling. Concurrently, TSC in the same-time point, inhibits pAMPK Thr172, triggering to decreased phosphorylation of ACC on Ser79 that increases its enzymatic activity, thus leading to an upregulated fatty acid synthesis.

Figure 10. Waist circumference (cm) at baseline and 12 months after the switch to OD-DR-HC

WC: baseline 99,31 ± 10,36 *vs* 12 months OD-DR-HC 95,9 ± 9 (p=0.004); *p<0.05

Figure 11. Area under the curve (AUC) for glucose (A) and insulin (B) at baseline and 12 months after the switch to OD-DR-HC in the subgroup of 11 patients evaluated with OGTT

AUC glucose*: baseline 14203,6 ± 3313,53 *vs* 12 months OD-DR-HC 12001,4 ± 3070,25 (p=0.014); AUC insulin*: baseline 12942,5 ± 6867,8 *vs* 12 months OD-DR-HC 6873,7 ± 3141,6 (p<0.05); *p<0.05

Figure 12. Insulin levels (µU/ml) 120' after OGTT at baseline and 12 months after the switch to OD-DR-HC in the subgroup of 11 patients evaluated with OGTT

Insulin 120' after OGTT: baseline 104,6 ± 50,7 vs 12 months OD-DR-HC 62,8 ± 49,7 (p<0.05); *p<0.05

Figure 13. Insulin Sensitivity Index, ISI0', at baseline and 12 months after the switch to OD-DR-HC in the subgroup of 11 patients evaluated with OGTT

ISI0': baseline 18,4 ± 8,9 *vs* 12 months OD-DR-HC 28,3 ± 15,7 (p=0.032); *p<0.05

Figure 14. Cortisol circadian rhythm explored by collecting serum cortisol blood samples (ng/ml) every three hrs both at baseline and 12 months after the switch to OD-DR-HC.

Serum Cortisol 7 pm: baseline 109,1± 87,2 *vs* 12 months OD-DR-HC 39,8 ± 18 (p=0.02)

Serum Cortisol 10 pm: baseline 64,3± 51,8 *vs* 12 months OD-DR-HC 29 ± 17,1 (p=0.029)

Figure 15. AUC (7 pm-1am) (A) and AUC (7 pm-7am) (B) explored by collecting serum cortisol blood samples (ng/ml) every three hrs both at baseline and 12 months after the switch to OD-DR-HC.

AUC4 (7 pm- 1 am): baseline 395,6± 254,6 *vs* 12 months OD-DR-HC 176,8 ± 87,6 (p=0.007); AUC8 (7 pm- 7 am): baseline 575,6 ± 297,1*vs* 12 months OD-DR-HC 358 ± 234,7 (p=0.035); *p<0.05

Figure 16. Counts of circulating CD14+ CD16- (A) and CD16+ CD14- (B) over time

Data are estimated marginal means and 95% CIs. Cell counts were measured at baseline (n=114), 12 weeks (n=108), and 24 weeks (n=103). Estimates were adjusted for age, sex, BMI, type of AI, diabetes, and smoking. (*Courtesy of Isidori A. M. Lancet Diabetes Endocrinol 2018*)

Figure 17. Concentrations of soluble CD16 and ADAM17

Circulating concentrations of soluble CD16 and ADAM17 were measured at baseline (n=114) and 12 weeks (n=108). The bottom of the boxplot indicates the 25th percentile and the top the 75th percentile. Horizontal lines in the boxes are medians. The lower end of the whiskers represents the minimum observation and the upper end the maximum. Treatment differences were derived from a mixed-effects analysis of covariance after adjusting for age, sex, BMI, type of AI, diabetes, and smoking. ADAM17=disintegrin and metalloproteinase domain-containing 17. (*Courtesy of Isidori A. M. Lancet Diabetes Endocrinol 2018*)

Table 1. Treatment schedule after C2C12 synchronization

Synchronized C2C12 cells have been treated with different concentrations of HC to mimic circulating cortisol concentrations observed in healthy human subjects and the serum cortisol peaks (expressed in nmol/L) in AI patients treated with once-daily MR-HC or thrice-daily IR-HC conventional treatments. 12 hrs post serum free medium replacement, corresponding to Bmal1 acrophase, resembled the 8 am in the daily rhythm; 15 hrs post

serum free medium replacement, corresponding to Bmal1 midphase, resembled the 1 pm in the daily rhythm; 18 hrs post serum free medium replacement, corresponding to Bmal1 bathyphase, resembled the 6 pm in the daily rhythm. TSA: treatment schedule A; TSB: treatment schedule B; TSC: treatment schedule C.

Table 2. Gene symbols and name of 21 genes significantly downregulated during bathyphase when TSA was compared to TSC

Table 3. Gene symbols and name of 22 genes significantly downregulated during bathyphase when TSB was compared to TSC

Figure 1.

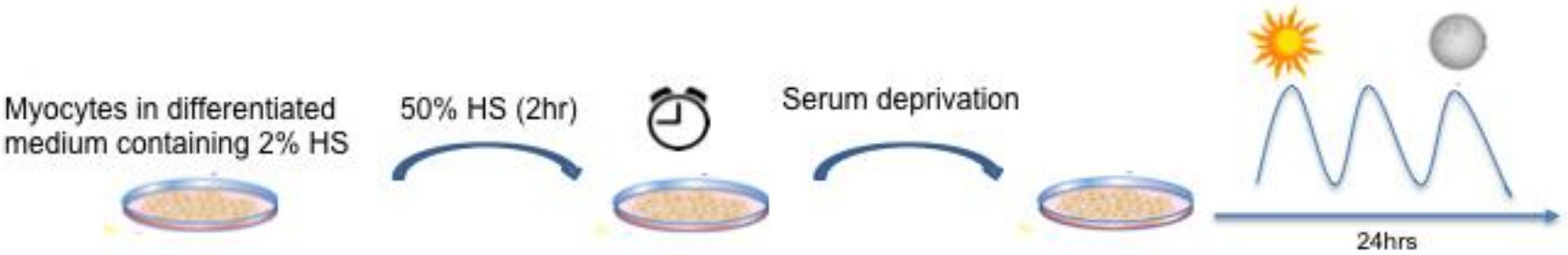
Myocytes in differentiated medium containing 2% HS
50% HS (2hr)
Serum deprivation
24hrs

Figure 2.

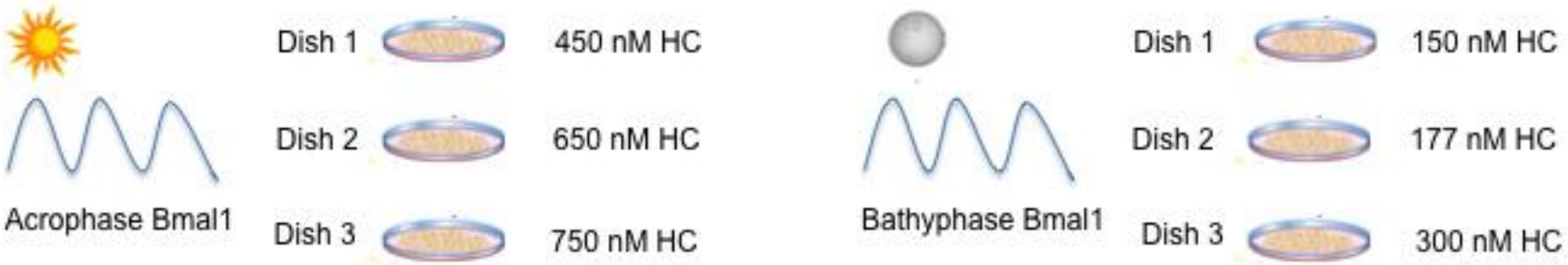
Dish 1
450 nM HC
Dish 2
650 nM HC
Acrophase Bmal1
Dish 3
750 nM HC
Dish 1
150 nM HC
Dish 2
177 nM HC
Bathyphase Bmal1
Dish 3
300 nM HC

Table 1.

Time-points		Hydrocortisone concentrations to recapitulate *in vitro* the serum cortisol patterns observed in patients under once daily MR-HC or thrice-daily IR-HC treatments (nmol/L)		
		TSA	**TSB**	**TSC**
Hrs after starvation	***Bmal1* gene expression**	**Physiological**	**MR-HC**	**IR-HC**
12	acrophase	400	650	750
15	midphase	200	372	600
18	bathyphase	150	177	300

Peaks concentration values and relative time points extrapolated by the serum cortisol profile obtained in normal individuals (reported by Debono et al. 2009) or in patients after conventional IR-HC treatment (reported in Johannsson et al. 2012). TSA: treatment schedule A; TSB: treatment schedule B; TSC: treatment schedule C.

Figure 3.

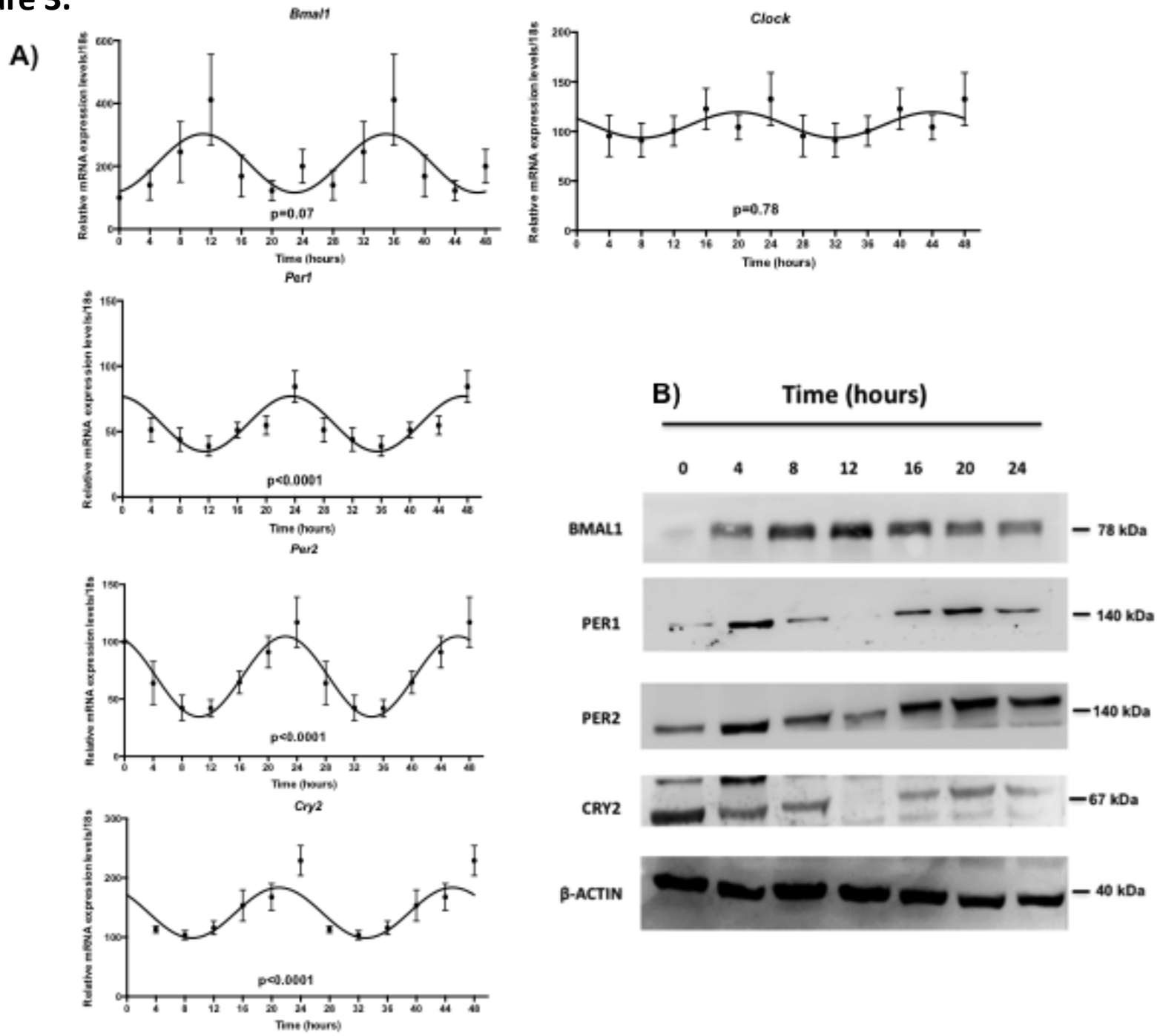
A)
Bmal1
Relative mRNA expression levels/18s
p=0.07
Time (hours)
Clock
Relative mRNA expression levels/18s
p=0.78
Time (hours)
Per1
Relative mRNA expression levels/18s
p<0.0001
Time (hours)
Per2
Relative mRNA expression levels/18s
p<0.0001
Time (hours)
Cry2
Relative mRNA expression levels/18s
p<0.0001
Time (hours)
B)
Time (hours)
0
4
8
12
16
20
24
BMAL1
78 kDa
PER1
140 kDa
PER2
140 kDa
CRY2
67 kDa
β-ACTIN
40 kDa

Figure 4.

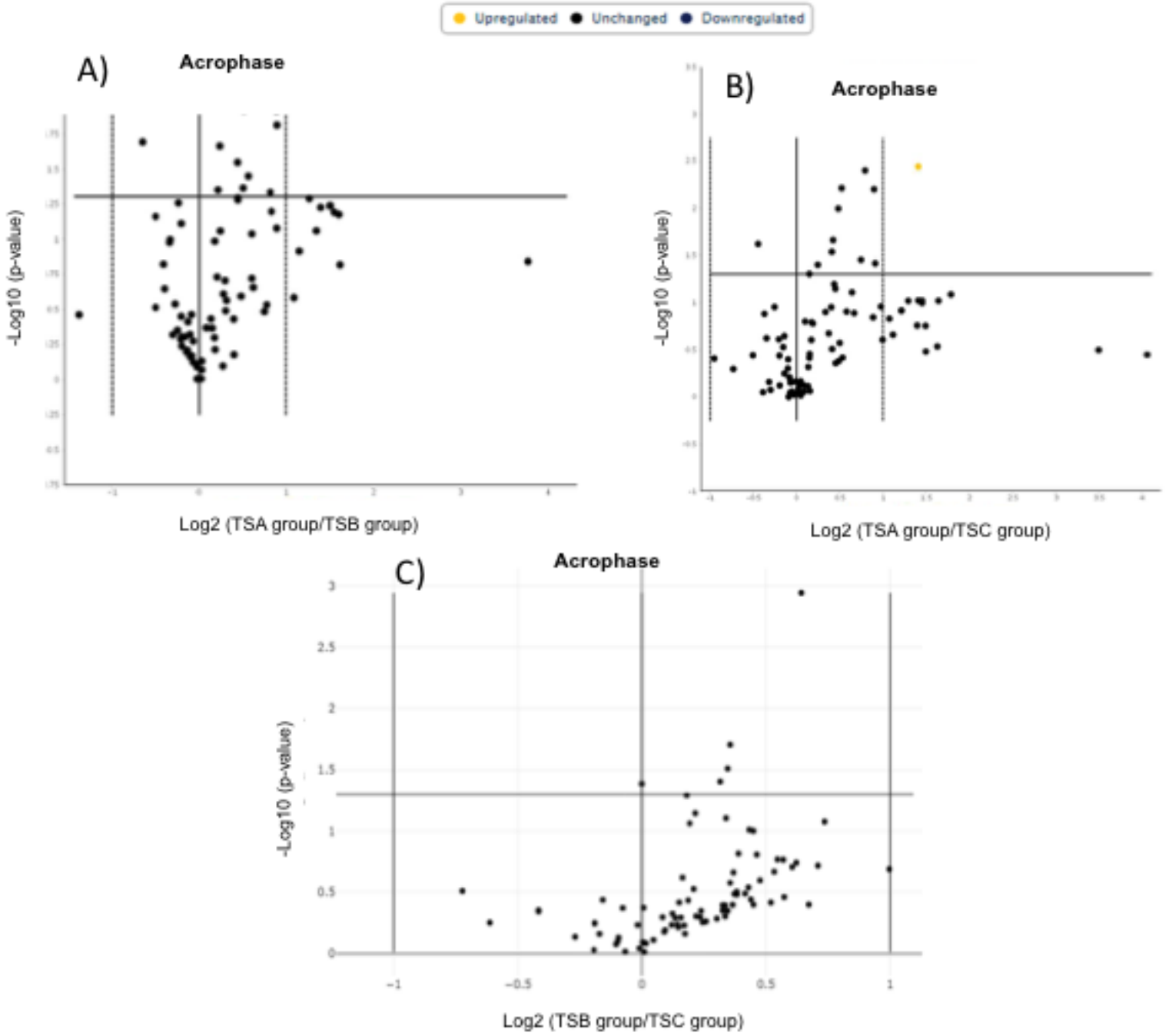
Upregulated
Unchanged
Downregulated
A)
Acrophase
-Log10 (p-value)
Log2 (TSA group/TSB group)
B)
Acrophase
-Log10 (p-value)
Log2 (TSA group/TSC group)
C)
Acrophase
-Log10 (p-value)
Log2 (TSB group/TSC group)

Figure 5.

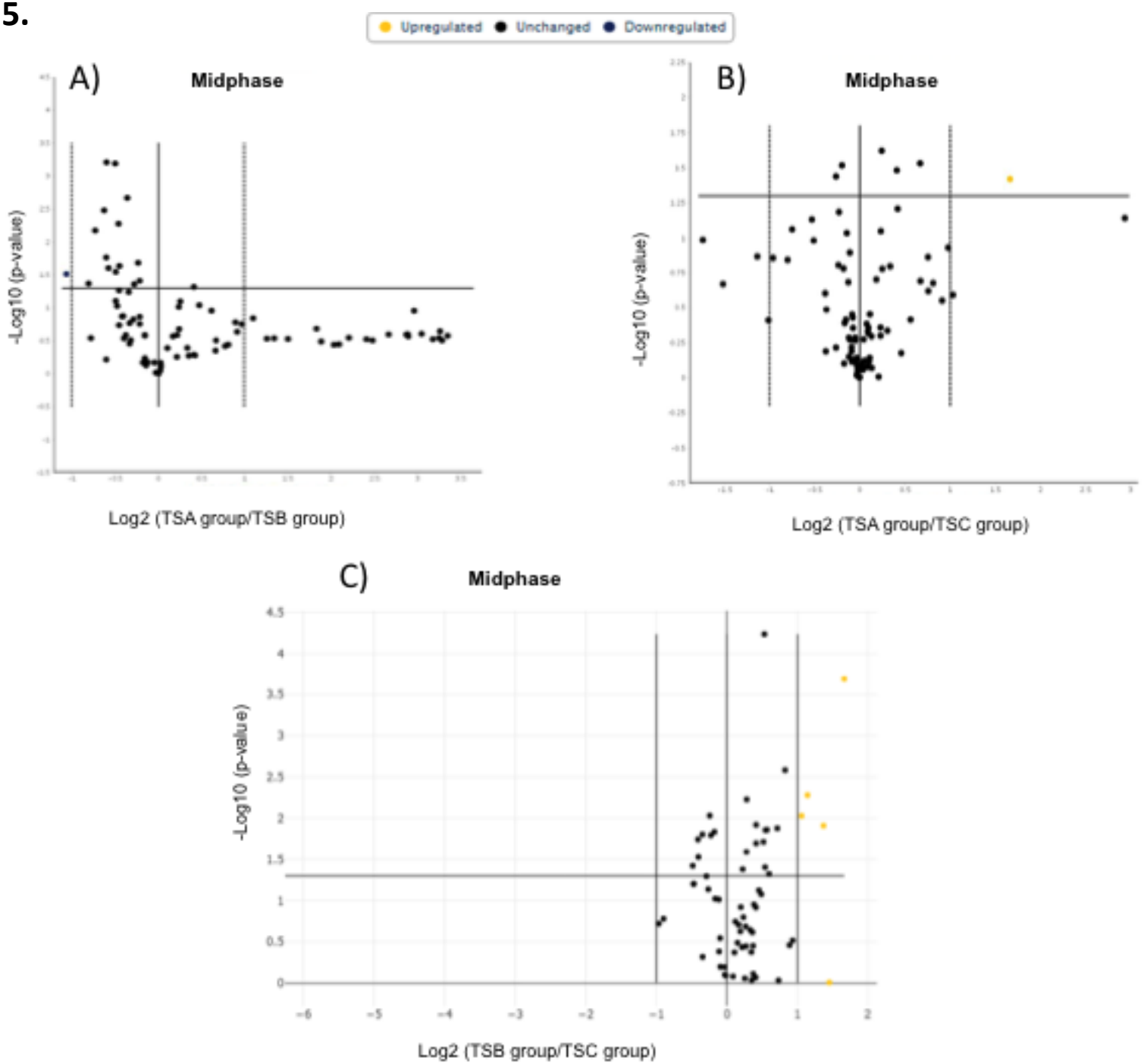
Upregulated
Unchanged
Downregulated
A)
Midphase
-Log10 (p-value)
Log2 (TSA group/TSB group)
B)
Midphase
-Log10 (p-value)
Log2 (TSA group/TSC group)
C)
Midphase
-Log10 (p-value)
Log2 (TSB group/TSC group)

Figure 6.

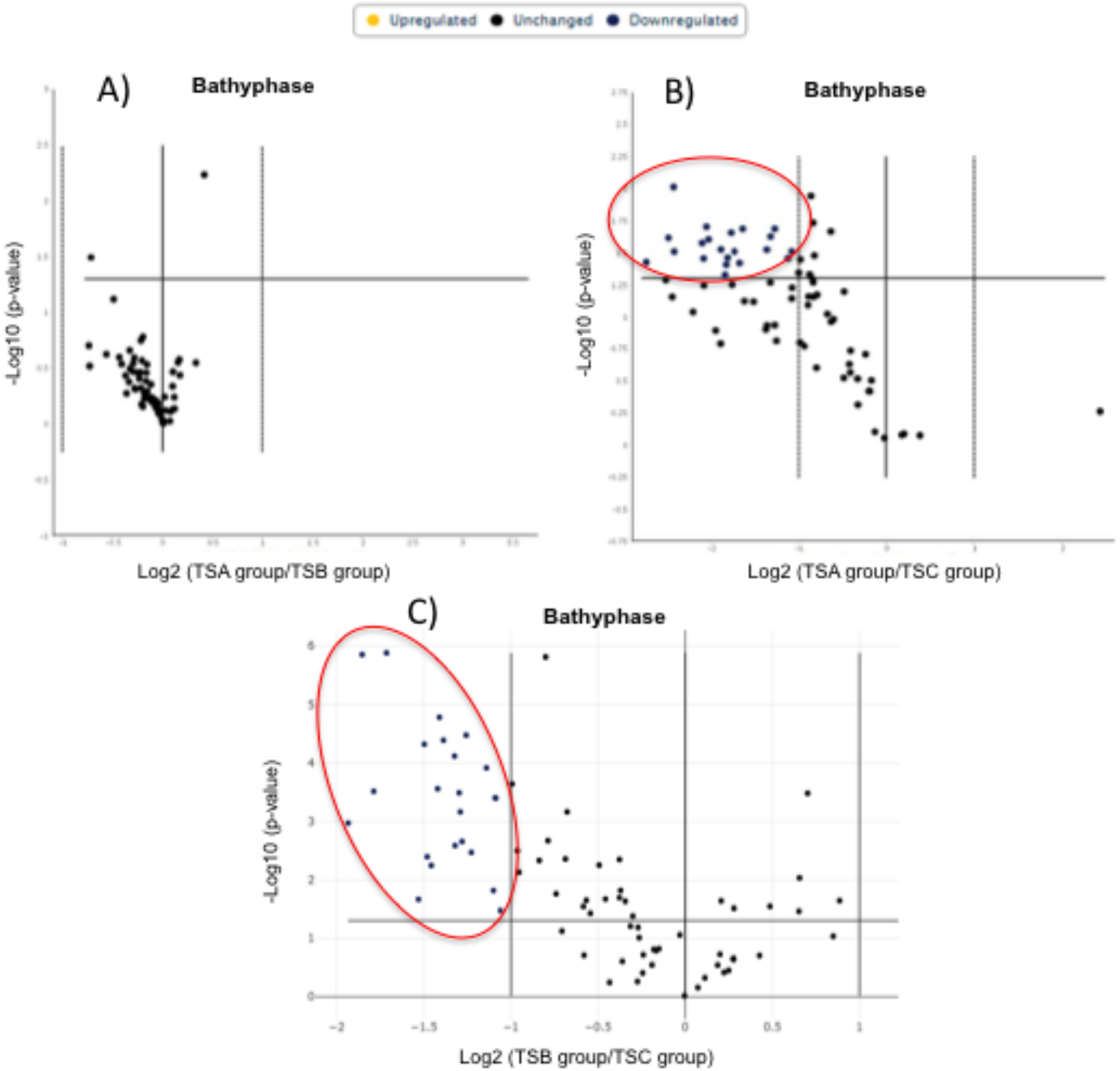
Upregulated
Unchanged
Downregulated
A)
Bathyphase
-Log10 (p-value)
Log2 (TSA group/TSB group)
B)
Bathyphase
-Log10 (p-value)
Log2 (TSA group/TSC group)
C)
Bathyphase
-Log10 (p-value)
Log2 (TSB group/TSC group)

Table 2.

Gene symbol	Gene name	Fold change	p-value
Acaca	Acetyl-CoA Carboxylase Alpha	-5.37	0.009718
Acacb	Acetyl-CoA Carboxylase Beta	-2.49	0.023602
Acsl4	Long-chain-fatty-acid—CoA ligase 4	-2.57	0.029905
Adipor2	Adipokine receptor 2	-3.70	0.029810
Alox5	Arachidonate 5- Lipoxygenase	-4.29	0.026506
Cebpa	CCAAT/enhancer binding protein alpha	-6.68	0.037441
Fasn	Fatty acid synthase	-2.42	0.020579
Ifng	Interferon gamma	-2.18	0.034901
Ikbkb	Inhibitor of nuclear factor kappa B kinase subunit beta	-4.25	0.034995
Il1r1	Interleukin 1 receptor	-3.59	0.046924
Insr	Insulin receptor	-5.60	0.024156
Irs1	Insulin receptor substrate 1	-4.15	0.019819
Irs2	Insulin receptor substrate 2	-3.32	0.030917
Lipe	Lipase E	-4.08	0.024886
Lta4h	Leukotriene A4 Hydorxylase	-3.11	0.020585
Mapk3	Mitogen-Activated Protein Kinase 3	-3.55	0.039112
Olr1	Oxidized low density lipoprotein receptor 1	-3.51	0.034575
Plk3ca	Phosphatidylinositol-4,5-bisphosphate 3-kinase catalytic subunit alpha	-2.11	0.030844
Socs3	Suppressor Of Cytokine Signaling 3	-3.19	0.038021
Stat3	Signal transducer and activator of transcription 3	-3.42	0.022028
Tnfraf1b	Tumor necrosis factor receptor superfamily, member 1b	-5.35	0.030947

Table 3.

Gene symbol	Gene name	Fold change	p-value
Acaca	Acetyl-CoA Carboxylase Alpha	**-2.75**	**0.005650**
Adipor2	Adipokine receptor 2	**-2.50**	**0.002580**
Alox5	Arachidonate 5- Lipoxygenase	**-2.09**	**0.033591**
Cebpa	CCAAT/enhancer binding protein alpha	**-3.82**	**0.001066**
Crlf2	Cytokine Receptor Like Factor 2	**-2.20**	**0.000122**
Cs	Citrate synthase	**-2.68**	**0.000276**
Hk2	Hexokinase 2	**-2.39**	**0.000034**
Ikbkb	Inhibitor of nuclear factor kappa B kinase subunit beta	**-2.82**	**0.000048**
Il1r1	Interleukin 1 receptor	**-2.50**	**0.000076**
Insr	Insulin receptor	**-3.28**	**0.000001**
Irs1	Insulin receptor substrate 1	**-2.45**	**0.000686**
Irs2	Insulin receptor substrate 2	**-2.12**	**0.000400**
Lipe	Lipase E	**-2.79**	**0.004016**
Lta4h	Leukotriene A4 Hydorxylase	**-2.13**	**0.000395**
Mapk3	Mitogen-Activated Protein Kinase 3	**-2.43**	**0.002200**
Mtor	mammalian target of Rapamycin	**-2.62**	**0.000041**
Olr1	Oxidized low density lipoprotein receptor 1	**-2.14**	**0.015128**
Pycard	Phosphatidylinositol-4,5-bisphosphate 3-kinase catalytic subunit alpha	**-2.89**	**0.021533**
Serpine1	Serine proteinase inhibitor 1	**-2.34**	**0.003379**
Slc27a1	Solute Carrier Family 27 Member 1	**-3.61**	**0.000001**
Socs3	Suppressor Of Cytokine Signaling 3	**-2.46**	**0.000324**
Stat3	Signal transducer and activator of transcription 3	**-2.66**	**0.000017**

Figure 7.

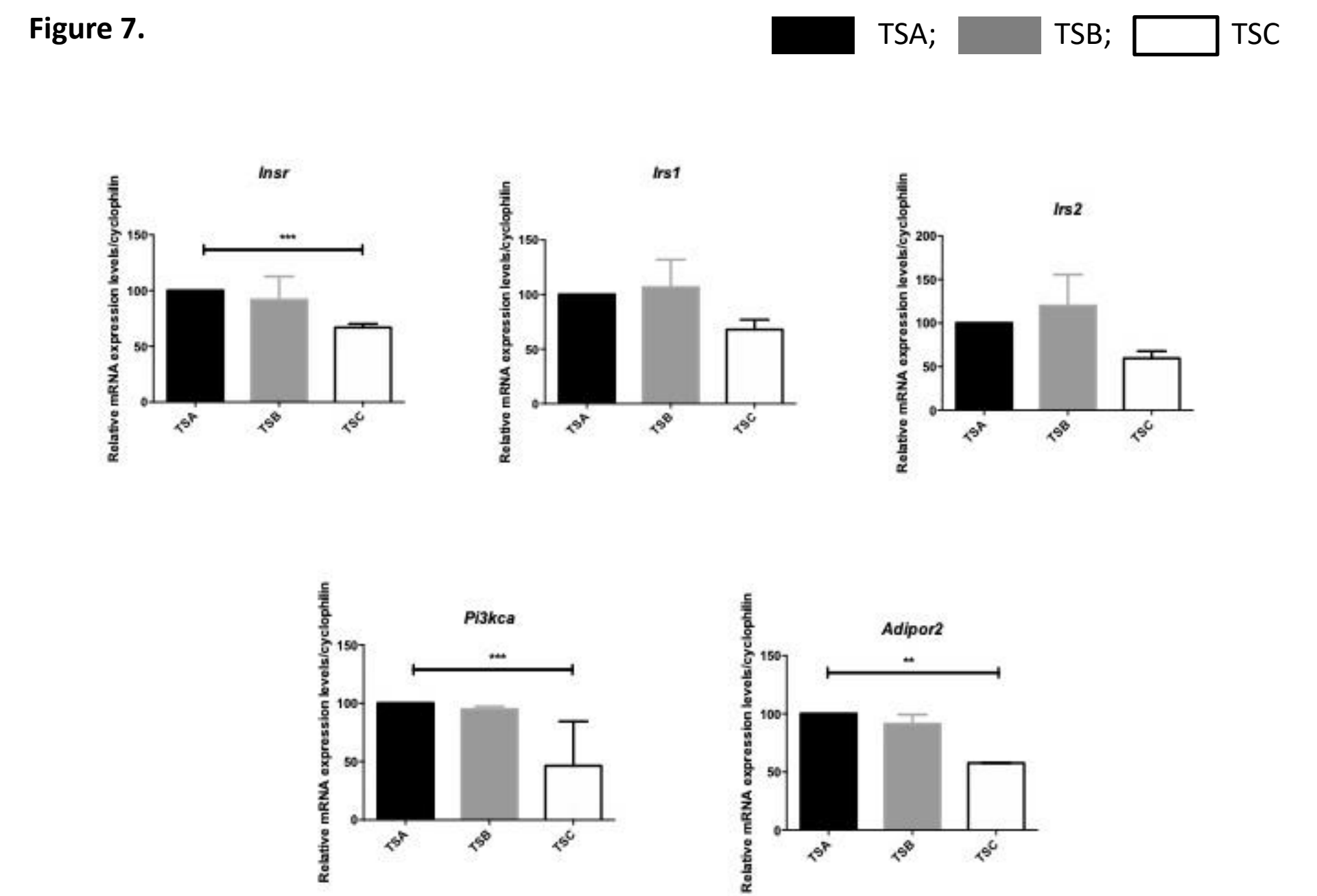
TSA;
TSB;
TSC
Insr
Irs1
Irs2
Pi3kca
Adipor2
Relative mRNA expression levels/cyclophilin
TSA
TSB
TSC
***
**

Figure 8.

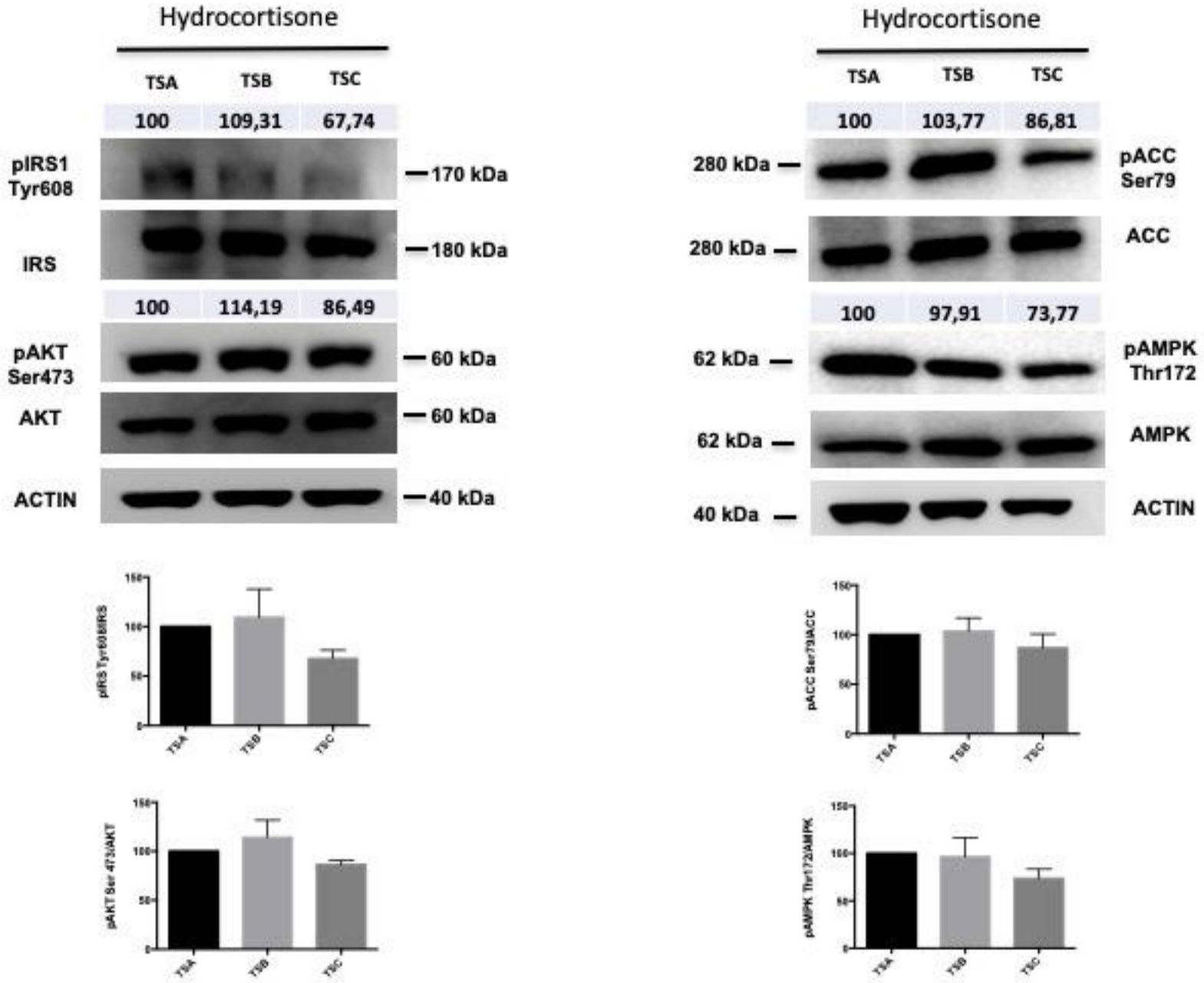
Hydrocortisone
TSA
TSB
TSC
100
109,31
67,74
pIRS1 Tyr608
170 kDa
IRS
180 kDa
100
114,19
86,49
pAKT Ser473
60 kDa
AKT
60 kDa
ACTIN
40 kDa
Hydrocortisone
TSA
TSB
TSC
100
103,77
86,81
280 kDa
pACC Ser79
280 kDa
ACC
100
97,91
73,77
62 kDa
pAMPK Thr172
62 kDa
AMPK
40 kDa
ACTIN
pIRS Tyr608/IRS
pACC Ser79/ACC
pAKT Ser 473/AKT
pAMPK Thr172/AMPK

Figure 9.

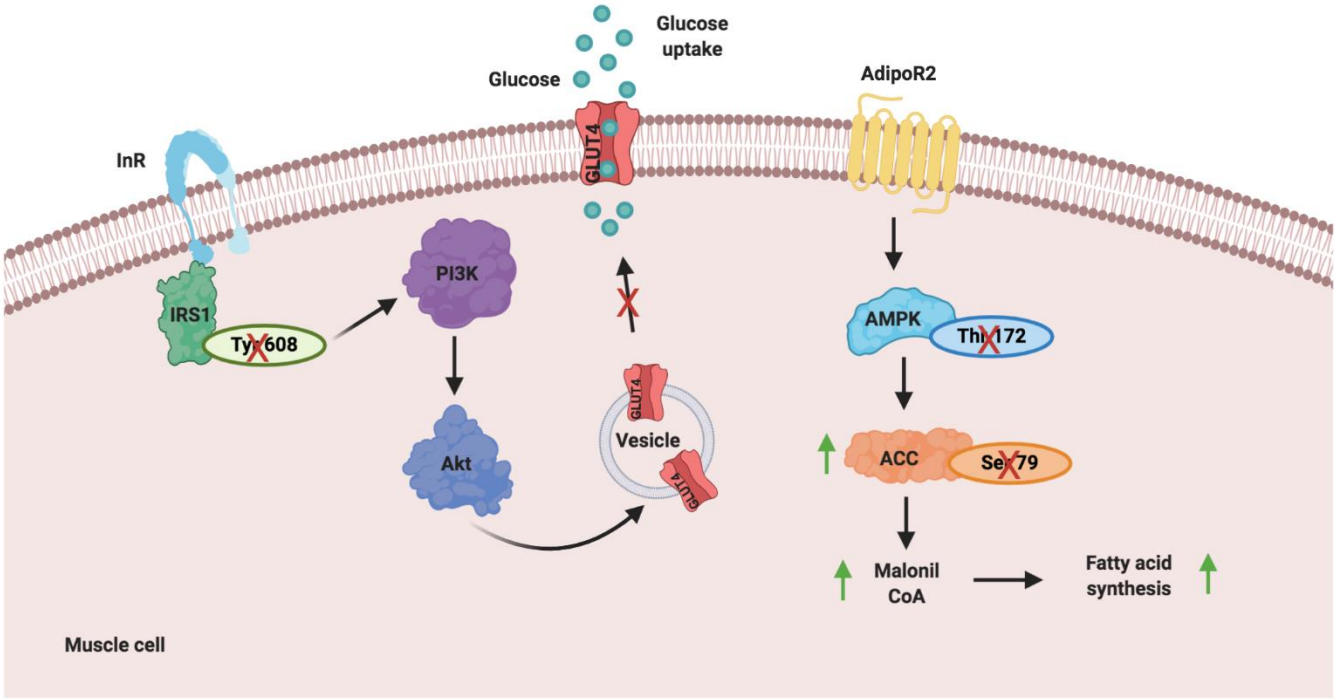
Glucose uptake
Glucose
GLUT4
AdipoR2
InR
IRS1
Tyr608
PI3K
Akt
Vesicle
GLUT4
GLUT4
AMPK
Thr172
ACC
Ser79
Malonil CoA
Fatty acid synthesis
Muscle cell

Figure 10.

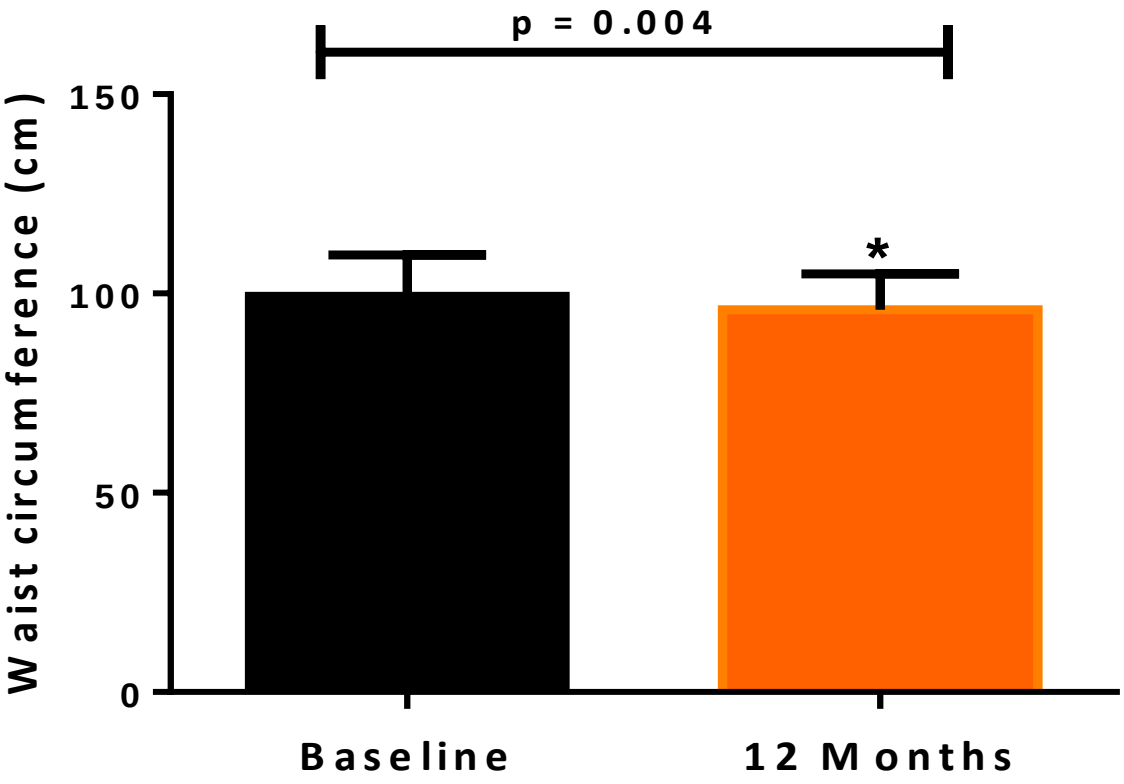
p = 0.004
Waist circumference (cm)
150
100
50
0
*
Baseline
12 Months

Figure 11.

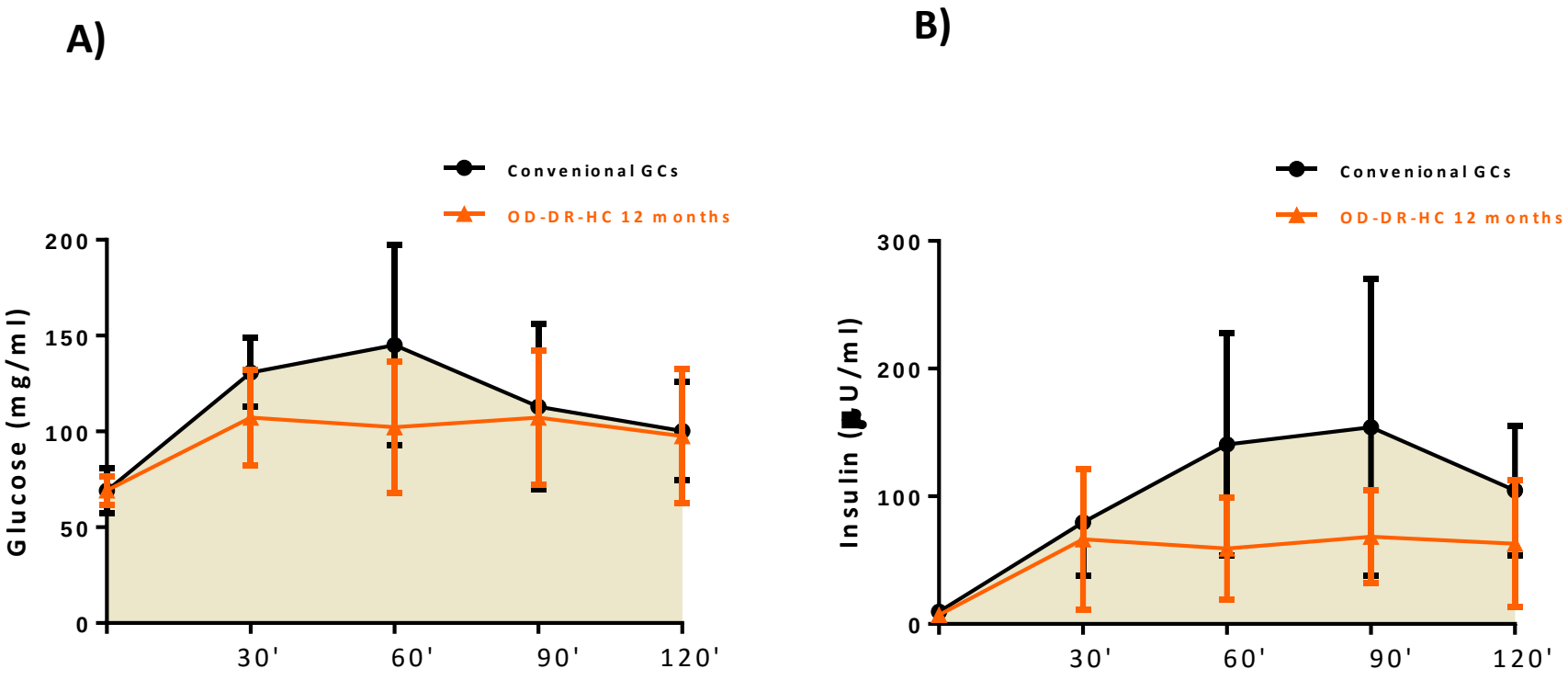
A)
Convenional GCs
OD-DR-HC 12 months
Glucose (mg/ml)
200
150
100
50
0
30'
60'
90'
120'
B)
Convenional GCs
OD-DR-HC 12 months
Insulin (µU/ml)
300
200
100
0
30'
60'
90'
120'

Figure 12.

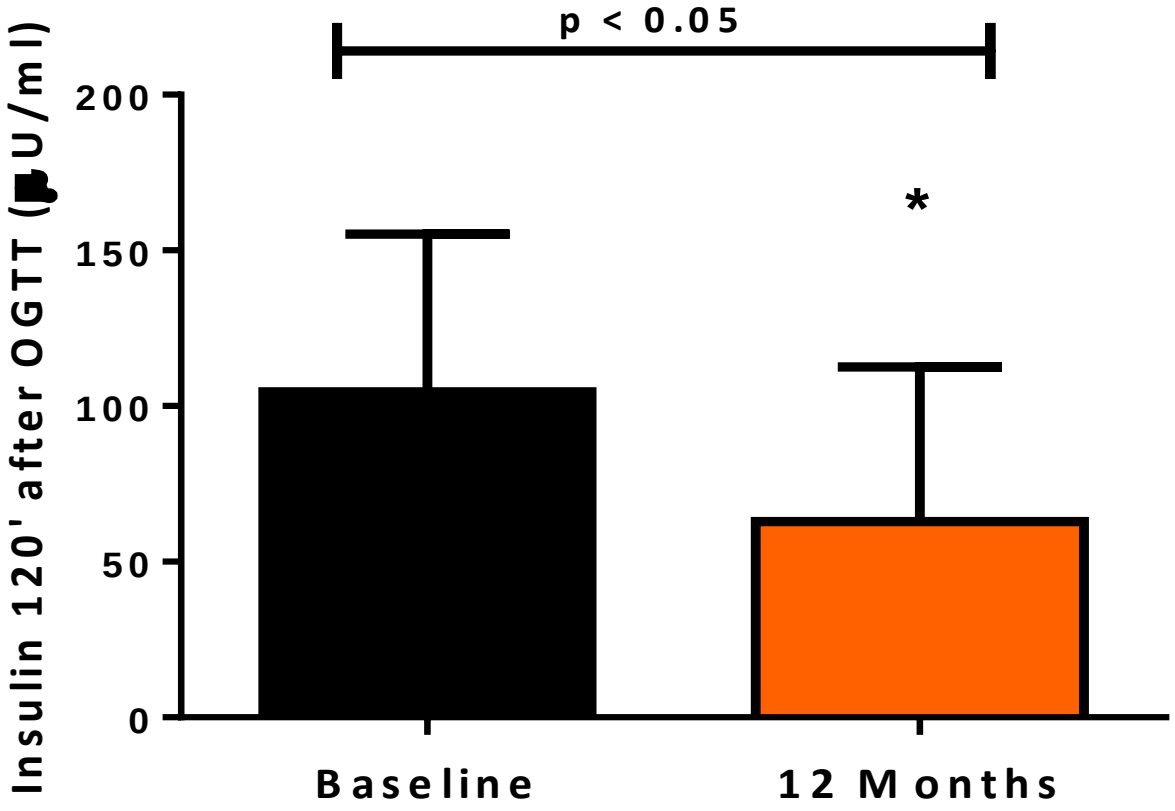
p < 0.05
Insulin 120' after OGTT (μU/ml)
200
150
100
50
0
*
Baseline
12 Months

Figure 13.

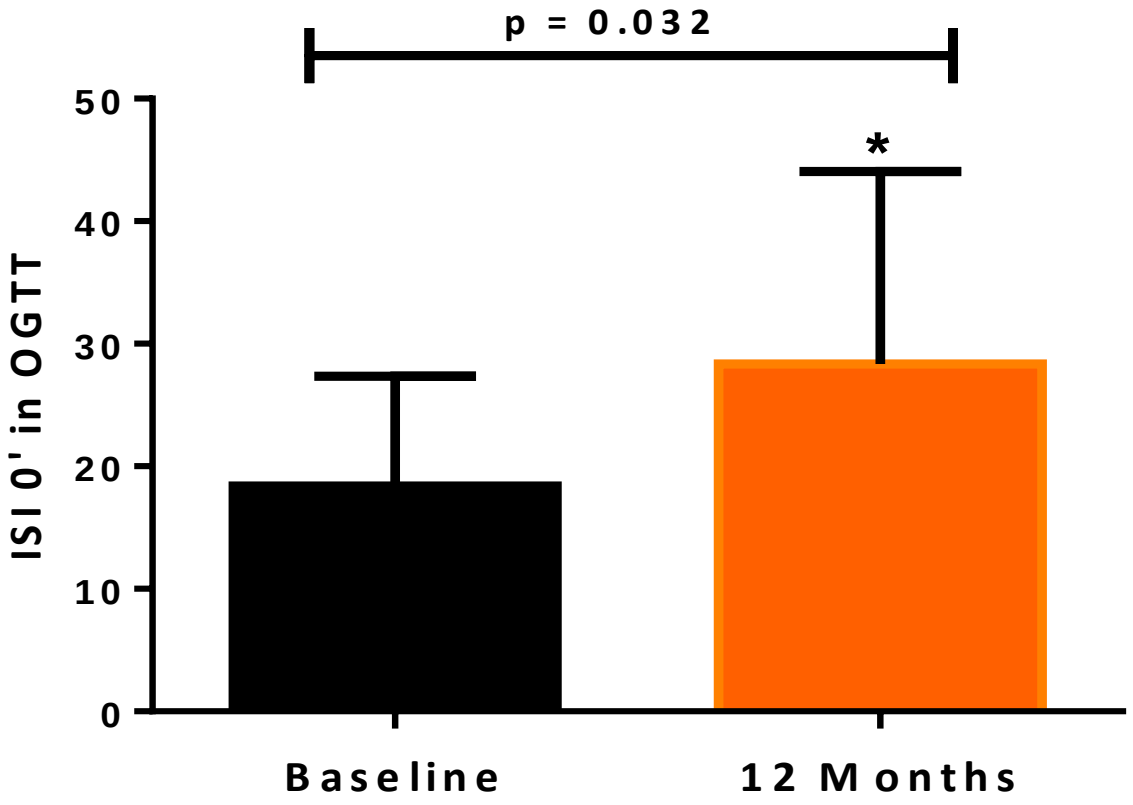

Figure 14.

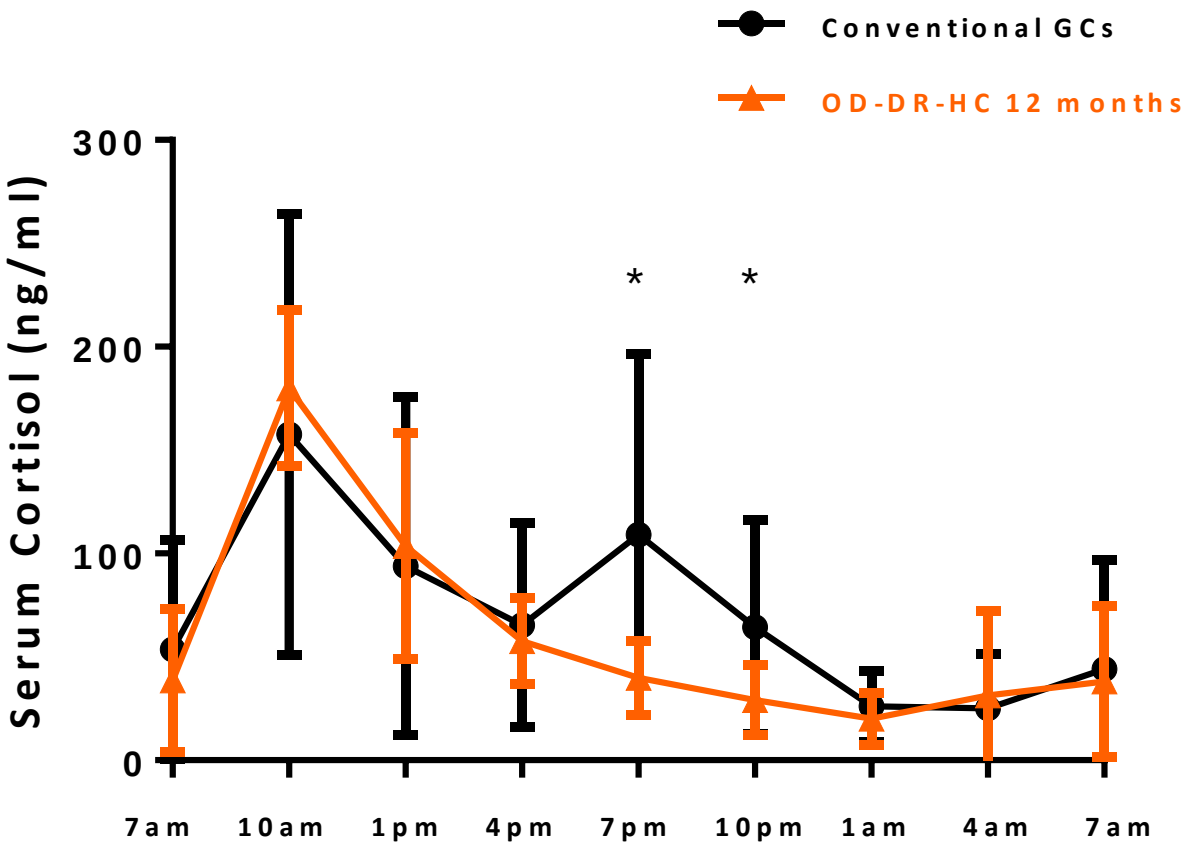
Conventional GCs
OD-DR-HC 12 months
Serum Cortisol (ng/ml)
300
200
100
0
*
*
7am
10am
1pm
4pm
7pm
10pm
1am
4am
7am

Figure 15.

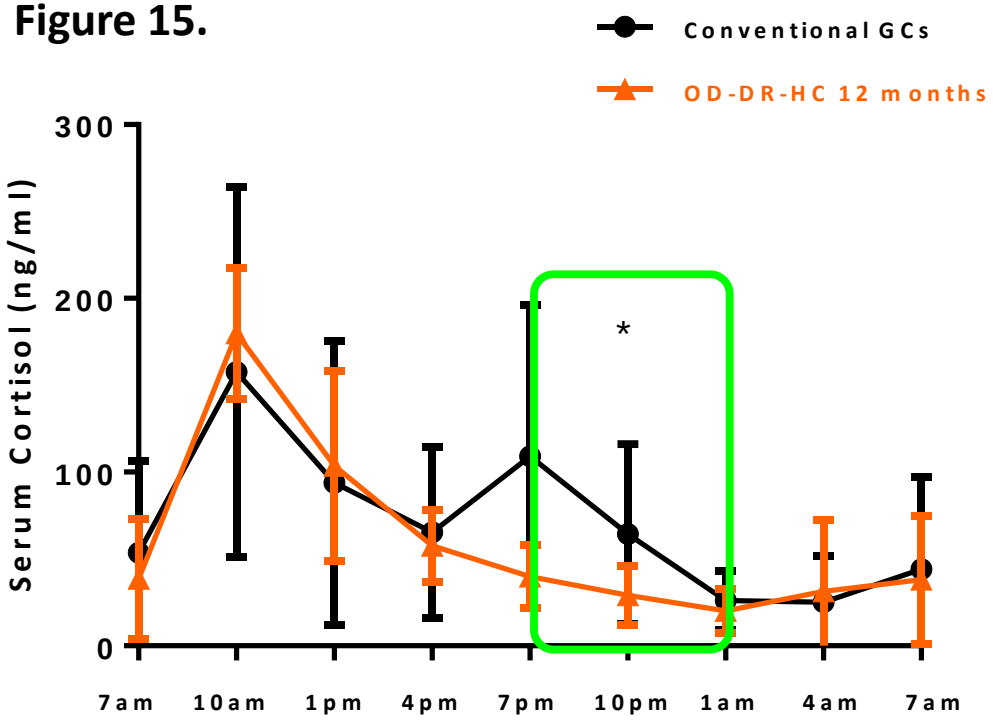
Conventional GCs
OD-DR-HC 12 months
Serum Cortisol (ng/ml)
300
200
100
0
*
7am
10am
1pm
4pm
7pm
10pm
1am
4am
7am

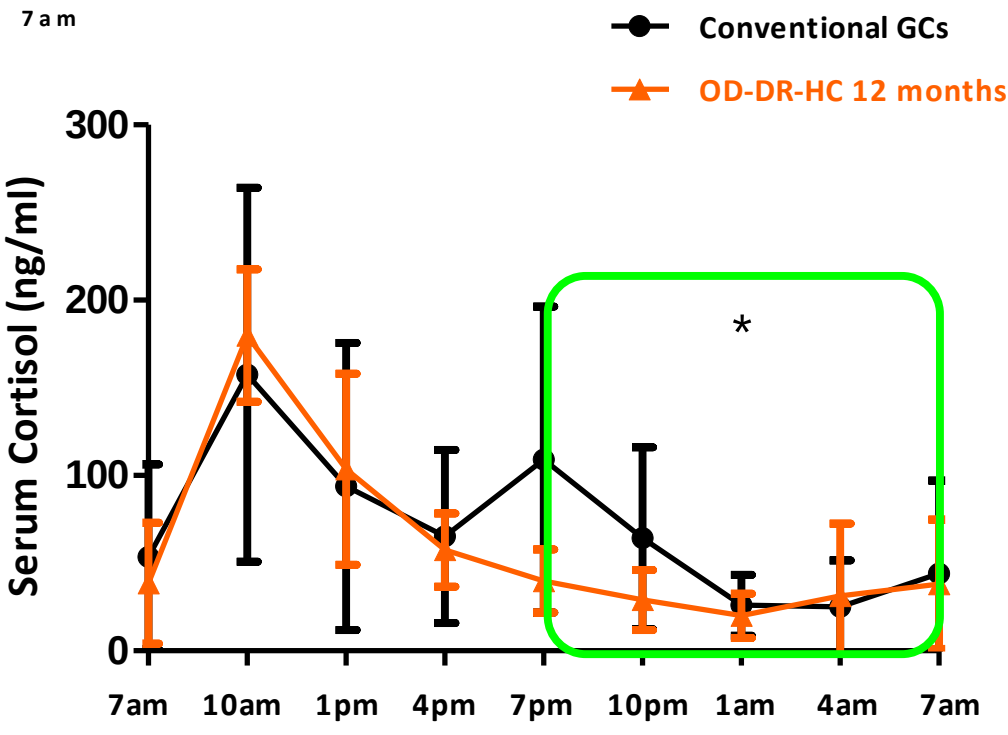
Conventional GCs
OD-DR-HC 12 months
Serum Cortisol (ng/ml)
300
200
100
0
*
7am
10am
1pm
4pm
7pm
10pm
1am
4am
7am

Figure 16.

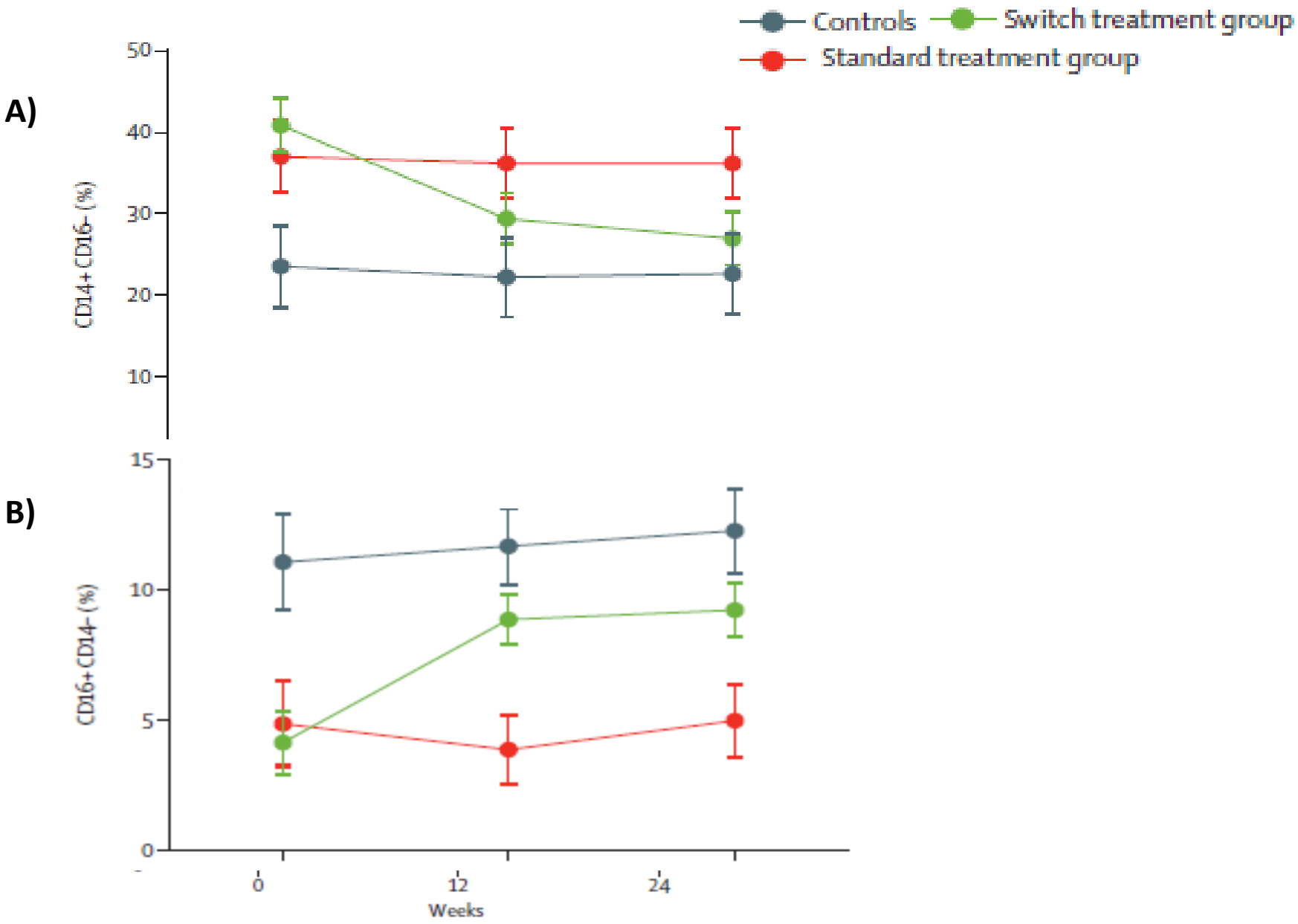
Controls
Switch treatment group
Standard treatment group
A)
B)
CD14+CD16- (%)
CD16+CD14- (%)
50
40
30
20
10
15
10
5
0
0
12
24
Weeks

Figure 17.

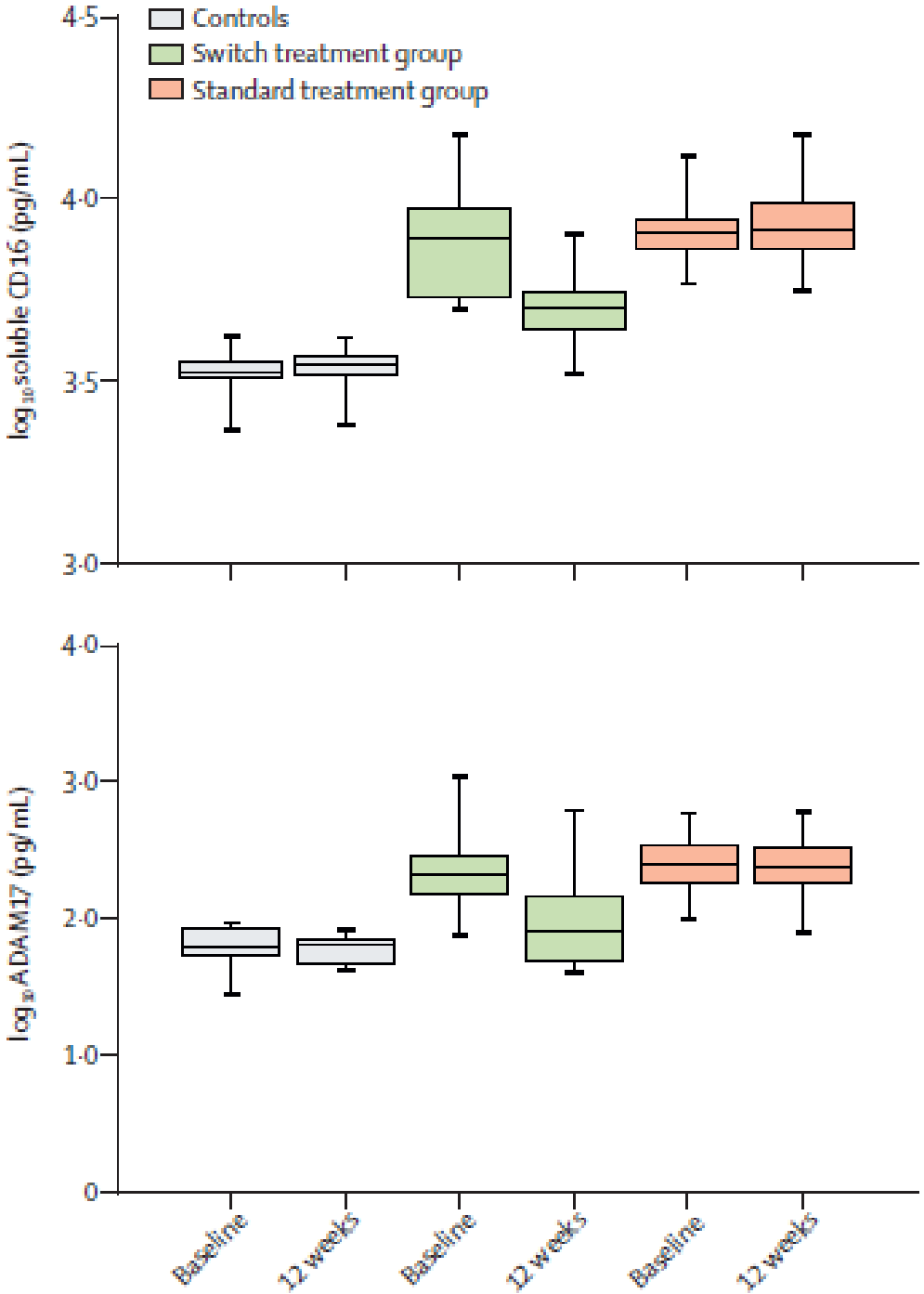
Controls
Switch treatment group
Standard treatment group
4·5
4·0
3·5
3·0
log10soluble CD16 (pg/mL)
4·0
3·0
2·0
1·0
0
log2ADAM17 (pg/mL)
Baseline
12 weeks
Baseline
12 weeks
Baseline
12 weeks